ON THE APPLICABILITY OF FIXED POINT THEORY TO THE DESIGN OF COUPLED CORE WALLS

by

Daniel H. Hull

B.S. in Civil Engineering, University of Pittsburgh, 2004

Submitted to the Graduate Faculty of

the School of Engineering in partial fulfillment

of the requirements for the degree of

Master of Science

University of Pittsburgh

2006

UNIVERSITY OF PITTSBURGH

SCHOOL OF ENGINEERING

This thesis was presented

by

Daniel H. Hull

It was defended on

April 4, 2006

and approved by

John Oyler, Adjunct Associate Professor,
Department of Civil and Environmental Engineering

Morteza Torkamani, Associate Professor,
Department of Civil and Environmental Engineering

Thesis Advisor: Kent Harries, Assistant Professor,
Department of Civil and Environmental Engineering

ON THE APPLICABILITY OF FIXED POINT THEORY TO THE DESIGN OF COUPLE CORE WALLS

Daniel H. Hull, M.S.

University of Pittsburgh, 2006

Coupled core walls offer an efficient lateral load resisting system. Due to their exceptional stiffness (many times greater than the sum of the component wall piers), coupled core wall structures are especially attractive in earthquake-resistant settings. Current design practice does not address dynamic properties of the structure, in particular the optimization of the coupling beams. The coupling beams affect both the "static" (stiffness) and dynamic performance of the structure to varying degrees depending on their damping and stiffness properties. Fixed Point Theory is applied to find optimal damping and stiffness values for beams coupling two wall pier structures. In this initial investigative work, "performance" is defined in a novel way: as the practical minimization of transmissibility of horizontal ground motion. An initial parametric study applies fixed point theory optimization to a series of 84 sets of wall piers. From this parametric study, two prototype structures are advanced and analyzed using linear time history analyses to assess their performance in a simulated earthquake. These "optimized" structures are compared to practical, uncoupled, and rigidly linked systems to determine the validity of the application of Fixed Point Theory to the choice of coupling beam properties.

TABLE OF CONTENTS

LIST OF TABLES

LIST OF FIGURES

NOMENCLATURE

The following symbols are used throughout this thesis. Where possible, notation taken from references was not changed from the original source documents.

A1	=	Wall 1 cross sectional area.
A2	=	Wall 2 cross sectional area.
E	=	Young's Modulus.
ek1	=	equivalent SDOF stiffness for Wall 1.
ek2	=	equivalent SDOF stiffness for Wall 2.
em1	=	equivalent SDOF mass for Wall 1.
em2	=	equivalent SDOF mass for Wall 2.
floors	=	Number of floors to model.
g	=	Coefficient from the closed form solution.
I1	=	Wall 1 moment of inertia.
I2	=	Wall 2 moment of inertia.
k	=	Optimal coupling beam stiffness.
K1	=	Wall 1 stiffness matrix.
k1	=	Story level stiffness of Wall 1.
K2	=	Wall 2 stiffness matrix.
k2	=	Story level stiffness of Wall 2.
h	=	Story height.
L	=	Coefficient from the closed form solution.
M1	=	Wall 1 mass matrix.
m1	=	Wall 1 story level mass.
M2	=	Wall 2 mass matrix.
m2	=	Wall 2 story level mass.

mtot	=	Total mass at the story level (m1 + m2).
rfloors	=	Floor level at which plastic hinge diminishes.
Sp	=	Coefficient for the natural frequency corresponding to the intersection point “P”.
Sp1	=	Component of the coefficient for the natural frequency corresponding to the intersection point “P”.
Sq	=	Coefficient for the natural frequency corresponding to the intersection point “Q”.
Sq1	=	Component of the coefficient for the natural frequency corresponding to the intersection point “Q”.
U	=	Lateral displacement.
U1	=	Lateral displacement to Wall 1.
U2	=	Lateral displacement to Wall 2.
$\alpha 1$	=	Stiffness coefficient for modification of EI to account for cracked section properties in plastic hinge region.
αu	=	Stiffness coefficient for modification of EI to account for cracked section properties outside the plastic hinge region.
γ	=	Frequency ratio of SDOF systems ($\omega 2 / \omega 1$).
$\Lambda 1$	=	Wall 1 eigenvalue matrix.
$\Lambda 2$	=	Wall 2 eigenvalue matrix.
μ	=	Mass ratio of Wall 2 to Wall 1 (m2 / m1).
ξ	=	Optimal coupling beam damping ratio (the average of ξA and ξB).
ξA	=	Fixed point damping ratio corresponding to the intersection point “P”, comprised of the following coefficients: aA, bA1, bA2, bA3a, bA3, bA4a, bA4, bA5a, bA5, bA, cA1, cA2, and cA.
ξB	=	The fixed point damping ratio corresponding to the intersection point “Q”, comprised of the following coefficients: aB, bB1, bB2, bB3a, bB3, bB4a, bB4, bB5a, bB5, bB, cB1, cB2, and cB.
η	=	Fixed point stiffness ratio (k / k1).
$\Phi 1$	=	Wall 1 eigenvector (mode shape) matrix.
$\varphi 1$	=	Normalized first mode shape vector for Wall 1.
$\Phi 2$	=	Wall 2 eigenvector (mode shape) matrix.
$\varphi 2$	=	Normalized first mode shape vector for Wall 2.

ω_1 = Natural frequency of Wall 1.

ω_2 = Natural frequency of Wall 2.

ω_{p1} = Component of the natural frequency corresponding to the intersection point "P".

ω_p = Natural frequency corresponding to the intersection point "P".

ω_{q1} = Component of the natural frequency corresponding to the intersection point "Q".

ω_q = Natural frequency corresponding to the intersection point "Q".

This document contains measurements and calculations using the International System (SI) of units. The following conversions apply:

1 inch	=	25.4 mm
1 foot	=	305 mm
1 kip	=	4.448 kN
1 ksi	=	6.895 MPa

Reinforcing bar sizes are reported using the standard inch-pound designation used in the United States designated by a '#' followed by a number referring to the bar diameter in eighths of an inch. Thus a #7 bar is a nominal 7/8 inch diameter bar.

ACKNOWLEDGEMENTS

The author would like to thank his advisor, Dr. Kent A. Harries, for his support, guidance, and patience as a teacher and advisor.

The author would also like to thank Dr. Andy Richardson of Post, Buckley, Schuh & Jernigan, Inc. (PBS&J) in Tampa Florida.

Finally, the author would like to thank his wife, Bethanné, for her patience and support during the completion of this thesis; his parents for their continued support of his academic growth; and his Lord and Savior, Jesus Christ - through Him, all things are possible.

1.0 INTRODUCTION

Coupled core wall (CCW) structures are very attractive design alternatives for earthquake resistant mid- and high-rise construction. Simply, a CCW consists of a series of cantilever wall piers coupled with moment resisting coupling beams (also called link beams). Practical design of these systems is complex and the peer-review process is often difficult to negotiate. The following comments are paraphrased from the experience of design engineers in designing CCWs (Shahrooz et al. 2006):

> *"Coupled walls are very commonly used, especially in high rise design, but there are many issues/challenges a designer must face."*
>
> *"Constructability is a huge issue. The diagonal reinforcing pattern combined with all of the ties and wall steel leave little room for tolerance, making placing nearly impossible in the real world. Relief on tie requirements will allow greater flexibility."*
>
> *"Upper bound to shear strength of* $10\sqrt{f'_c}bd$ [psi units] *is a constant issue. Many coupling beams are pushed to this limit considering code level seismic forces. Options for exceeding this limit are needed."*
>
> *"There is little guidance in North America for stiffness assumptions for different demand levels - wind, service earthquake, maximum considered earthquake."*

The basic information required to overcome these issues through development and implementation of performance-based design methods and/or innovative systems, does not exist or is very limited. A significant limitation in CCW design is the lack of any "rules of thumb" or relatively simple methods for establishing initial trial designs.

Harries (2001) demonstrated that idealized CCW analyses reported in the literature appeared to have excellent global structural behavior however the individual component response required to achieve this behavior was not justified based on existing experimental literature. Harries et al. (2004a) conducted an extensive parametric study of the elastic behavior

of 2016 idealized CCW structures and demonstrated significant force and displacement demands on coupling beams that could not be practically designed for or resisted.

It is felt that a performance-based design (PBD) approach may help to address many of these shortcomings in the design of CCW structures. In this work, "performance" will be defined in a novel way: as the ***practical minimization of transmissibility of horizontal ground motion***. Such an approach has not been tried and this thesis represents an exploratory study.

1.1 OBJECTIVES

The objective of the work presented in this thesis is to explore the application of Fixed Point Theory for establishing the practical minimization of transmissibility of horizontal ground motion in a coupled core wall structure. Fixed Point Theory will be used to establish initial design values for the coupling beams required to optimize the dynamic response of the entire CCW system. This work is exploratory in nature and therefore relies on a number of simplifications and idealizations described throughout the text.

1.2 OUTLINE

This thesis will cover the background subjects of coupled core walls, the generation of equivalent single degree of freedom (SDOF) systems, and fixed point theory in Chapter 2. In Chapter 3, a specific set of coupled core walls is reduced to two equivalent SDOF systems and the optimal coupling stiffness and damping values are found using fixed point theory. Chapter 4 covers the modeling and linear time history analysis for several scenarios for two sets of wall combinations. The conclusions and recommendations for future work are listed in Chapter 5.

2.0 LITERATURE REVIEW

The objective of this thesis is to apply Fixed Point Theory to the initial design of coupled wall structures. This chapter presents background material on the three major concepts on which this work is founded: coupled core wall structures, equivalent single degree of freedom systems, and fixed point theory. Knowledge and understanding of these concepts is essential to the development and analysis of the parametric study.

2.1 COUPLED CORE WALL STRUCTURES

Coupled core wall (CCW) structures resist applied lateral loads in an efficient manner through the coupling of individual wall piers to generate "frame" action between the walls in addition to the resistance provided by the flexural response of each cantilever pier. Core walls typically form the elevator shafts and are most often located in the center of the structure to maximize floor space. In the simplest scenario (and the one considered in the present work) a surrounding steel frame is used to carry the gravity loads, while the core walls are assumed to resist 100% the lateral loading (and its tributary share of the gravity loads). The walls and coupling beams are typically constructed of concrete, allowing the structure to perform well under fire or other catastrophic conditions. Concrete core structures are preferred for their toughness and their ability to protect the integrity of the primary egress (stairwells) for long periods of time in these conditions. Due to their exceptional stiffness, many times greater than the sum of the component wall piers, CCW structures are especially attractive in earthquake-resistant construction (Paulay, 1971).

When a structure consisting of a collection of uncoupled individual wall piers is loaded, the walls resist loading separately as cantilever walls. In CCW structures the wall piers are

coupled, usually at the story level, with connecting moment resisting coupling beams. As the walls are coupled, a system is created in which the walls act together to resist the lateral loading at varying degrees of efficiency based on the mechanical and physical properties of the connecting coupling beams. In this system, the coupled wall behavior approaches that in which the wall piers work together as one composite cantilever, rather than individual cantilevers, utilizing the increased moment arm from the centroid of the wall group to resist bending from applied lateral loads. The additional bending resistance is generated by the "frame action" introduced by the coupling beams resulting in an axial couple (tension and compression) being generated in the wall piers. This coupled system may be very efficient due to the large moment arm typically available. In a hypothetical fully composite system, the wall piers experience either axial tension or compression, while the uncoupled system, without frame action, contains wall piers that have a linear stress distribution as the lateral loads are resisted only by wall pier flexure. This is shown schematically in Figure 2.1 (Stafford-Smith and Coull, 1991).

As the wall piers deflect under a lateral loading, they rotate at each story level. The moment connection between the coupling beams and wall pier cause the beams to deflect in double curvature. For optimal structural performance, it is also assumed that all coupling beams yield prior to hinges forming at the bases of the wall piers (Harries and McNeice, 2006). The beam double curvature results in bending and shear reactions at the wall face that counter the tendency of the individual walls to rotate at the story level. The cumulative effect of these deformations and reactions of the connecting beams on the core walls greatly increases the axial forces that must be resisted by the wall piers. In a pushover scenario, the leading wall experiences greater compression forces while the trailing wall experiences tension. The increased tension is of greatest concern in that it is not generally desirable for this tension to overcome gravity (compression) loads at the wall base. If this occurs, the wall base and foundation must be designed for uplift. The increased compressive force on the leading wall is generally not a concern in design unless the wall piers are very slender, although it may result in the need for additional confining reinforcing details (ACI 318, 2005).

The efficiency of the coupled structure is described by the extent to which the structure behaves as a composite cantilever; that is the magnitude of the "frame action" described above. This efficiency is described as the degree of coupling (*doc*) of the CCW system. The *doc* can range from 0%, which represents core walls without coupling (linear stress distribution in the

walls), to 100%, in which the core walls are essentially doweled together by infinitely stiff beams, creating the hypothetical fully composite cantilever described above. The structural combination of the wall piers and the connecting beam is similar to a moment frame. The degree of coupling (*doc*) is defined as "the ratio of the overturning moment resisted by the 'frame' action to the total overturning moment" (Harries et al., 2004a) and is numerically defined as:

$$doc = \frac{N \cdot L_w}{\sum M_w + N \cdot L_w} \tag{2.1}$$

Where N is the axial load imparted to the wall pier from the accumulated shears of the coupling beams, L_w is the moment arm between the centroids of the walls, and M_w is the overturning moment resisted by each wall pier. Thus the denominator of Equation 2.1 represents the total overturning moment acting on the CCW structure.

In addition to vertical interaction effects, horizontal axial forces in the coupling beams themselves are generated in CCW structures. These forces result from the redistribution of horizontal shear forces from one wall pier to the other. Under lateral load, the "compression wall" naturally becomes stiffer while the "tension wall" is less capable of resisting moment and shear forces. Thus the overturning moment and lateral shear forces are redistributed from the tension wall to the compression wall. This redistribution is manifested as axial interaction forces in the coupling beams.

The design engineer must consider the practicality, constructability, and cost of the required beam properties and dimensions and weigh them against the desired design criteria and level of efficiency. Additionally, as noted, wall pier tension forces require considerable attention. A fully composite structure is impractical because the coupling beams would need an extremely stiff design. Since concrete is desirable for the design, the beam depth would be excessive, or the walls would have to be so close together that the benefits of coupling are lost. A design must be completed that satisfies normal design criteria (either performance or strength based design) and is practical for purposes of achieving dynamic properties of the structure (stiffness and damping). In this regard, Harries (2001) clearly demonstrated that it is often not possible to achieve the desired or predicted global CCW performance as the demands on the coupling beams greatly exceed their (experimentally demonstrated) capacity. Additionally, Harries et al. (2005) demonstrate that the code-compliant strength-based design of coupling beams often leads to unconstructable details.

2.1.1 Implications of CCW Behavior in the Context of the Present Work

As will be discussed, the dynamic behavior of CCWs is complex. This behavior, as measured by the stiffness and damping properties of each wall pier, varies tremendously even in a single seismic event. The interaction of the tension-compression couple described above results in the proportional stiffness of the wall piers shifting in favor of the compression wall. Damping, although more complex, likely increases in the tension wall. Similarly, axial interaction forces in the coupling beams are dominantly compressive near the base of the structure and tensile in the upper stories affecting the distribution of coupling beam forces and, again, the dynamic behavior of the structure.

2.1.2 Performance Based Design

Current design practice (ACI 318, 2005) utilizes strength based design (SBD). SBD entails the determination of likely loading on a structure and subsequently designing the structural members to resist that loading. Structural deflections are also checked, to ensure that they are within specified limits, although this is typically a post-design check. Performance based design (PBD) is very different from SBD. PBD uses criteria relating to the performance of a building or its structural members under user specified conditions to serve as the goals of the design. In "standard" terminology: PBD considers a spectrum of *performance objectives* under a spectrum of *performance levels* (or *hazard levels* in the case of seismic design). Performance objectives may pertain to desired yield mechanisms, constructability, or to the post-earthquake condition of the building (among other objectives), and may include specific criteria such as acceptable deflection limits during an earthquake. Performance levels relate to the hazard considered; in the case of seismic design, hazards are defined by the return periods or probabilities of exceedance of events having specific magnitudes. Once performance goals are set, the design team works to ensure that structural and member behavior are provided to meet the goals defined. PBD is often a two (or multiple) level design methodology where a design is executed at a "design" level hazard where the structure is expected to meet particular performance objectives. From this basis, the structural performance is verified at greater hazard levels where performance

objectives are not as stringent; or at reduced hazard levels where one may desire improved performance.

Performance objectives and hazard levels are set by the project owner and design team with guidance and minimum objectives defined by building codes and standards. One set of earthquake based performance objectives are the Target Building Performance Levels, which are laid out in FEMA 356 (2000). FEMA 356 is written as a pre-standard for the rehabilitation of structures, but the concept of PBD is well defined in this document and is applicable to new structures (though new structures are beyond the pre-standard's scope). While PBD is currently not used throughout the United States, it is in the process of being adopted by FEMA in this pre-standard. Additionally, Section 9.5.8 of ASCE 7-02 which permits non-linear dynamic time history analyses as an alternative method for determining seismic design and performance, appears to indicate a move toward PDB. In seismic practice today, some practitioners use a PBD approach coupled with a SBD presentation in order to satisfy SBD-based peer- and design-review requirements.

PBD requires the consideration of a hazard level. Four anticipated earthquake hazard levels were used to develop the criteria set forth for the performance levels prescribed by FEMA 356 (2000): *frequent* events, which have a 50% probability of exceedance in 50 years, *occasional* events (20%/50 years), *rare* events (10%/50 years), and *very rare* events (2%/50 years). Existing standards (ASCE 7-02, FEMA 356, etc) generally set their "design level" event as the 10%/50 year event and the "maximum credible" event as the 2%/50 year event. These are referred to as the design basis earthquake (DBE) and maximum credible earthquake (MCE), respectively.

Having established a hazard level, the target performance level chosen by the owner consists of a combination of a Structural Performance Level and a Nonstructural Performance Level (FEMA 356, 2000). The spectrum of structural performance levels is defined at discrete levels and intermediate ranges. The discrete levels are the Operational, Immediate Occupancy (IO), Life Safety (LS), Collapse Prevention (CP), and Not Considered (NC) levels. The intermediate ranges fall between these levels are referred to as Damage Control (between IO and LS) and Limited Safety (between LS and CP) ranges. In new construction NC is not applicable and will not be discussed further. The definitions of structural performance levels are paraphrased from FEMA 356:

Immediate Occupancy (S-1) - Light damage. Following an earthquake, the structure is safe to occupy with no remedial measures. The building's strength remains very close to the original design strength.

Life Safety (S-3) - Moderate damage. Structural damage is expected although none does not affect the life safety of the occupants nor restricts reasonable egress. The structure maintains significant reserve capacity to prevent partial or total collapse. Typically, damage is repairable.

Collapse Prevention (S-5) - Severe damage. Extensive structural damage is expected and casualties are possible – nonetheless a catastrophic collapse is not imminent; that is: the structural members have sufficient reserve capacity ***during*** and ***following*** the event to resist gravity loads. The building is near collapse and is not likely to be repairable.

Damage Control Range (S-2) and Limited Safety Range (S-4) are levels of performance obtained from the interpolation between the criteria of levels S1 and S3 and S3 and S5, respectively. Tables C1-3 and C1-4 in FEMA 356 (2000) provide relatively extensive guidance as to the specific nature of damage, story drifts, and other performance criteria expected at each performance level.

Similar criteria are defined for nonstructural performance levels (FEMA 356, 2000): Operational (N-A; non-structural elements in the building are able to function as well as they had before the earthquake), Immediate Occupancy (N-B; systems pertaining to access, egress, and mobility throughout the building remain intact and operable), Life Safety (N-C; damage is not life threatening), and Hazards Reduced (N-D; large, heavy objects are secure from falling, other building functions pertaining to access or fire protection not addressed). Non-structural performance criteria are described in Tables C1-5, C1-6, and C1-7 in FEMA 356.

Structural and non-structural performance levels are combined to determine the building's performance objective. In new construction, the levels are consistent and typically represented as one of three target performance levels: Immediate Occupancy (IO), Life Safety (LS), and Collapse Prevention (CP). Each performance level is assigned a hazard level. Thus the final structural performance is conventionally defined as: LS at the BDE event ***and*** CP at the MCE event. In some cases, a third reduced performance level is considered: often IO at the 20%/50 year or 50%/50 year event. From a practical standpoint, design is carried out at one level

(LS at DBE) and performance is verified at the others. Often some additional design or detailing is required to achieve CP and/or IO performance.

2.1.3 Performance Based Design of CCWs

When performance based design is adapted for CCW structures, it is appropriate to address another type of performance criteria relating to the desired behavior and progression of hinge development in the building. Specifically, it is desirable to ensure that all coupling beams yield prior to hinges forming at the wall pier bases. This behavior is similar to the strong column-weak girder design philosophy for ductile moment resisting frames (Paulay 1971; Park and Paulay 1975). Harries et al. (2005) also identify the design of constructible reinforced concrete coupling beams as a key initial consideration in the PDB of CCWs.

CCWs are "dual systems" – cantilever wall flexural behavior and "frame" action. The desired performance of the structure may therefore include the exhibition of different behaviors at different performance levels. For example: at the LS performance level, the structure could be considered a CCW, while at CP, it may be more desirable to assume the coupling beam capacity has degraded completely, resulting in loss of "frame" action, but respecting the CP performance goals of maintaining gravity load carrying capacity and reasonable evacuation of the structure (Harries et al., 2004b). This particular performance level is believed to address limitations in coupling beam performance identified by Harries (2001). Additionally, this progression of performance with increasing hazards is a major premise behind the work presented here.

A design methodology specific to CCW structures has been proposed by Harries et al. (2004b). This five step process is outlined as follows:

1. Definition of the performance objectives – This process, as described above, may be guided by FEMA 356 or from other reasonable and practical conditions.
2. Design constructible coupling beams that meet other performance criteria. With coupling beam design, it is essential that careful attention to shear details is maintained. While concrete is highly desirable for this application, other forms have been researched utilizing steel, hybrid sections, or fused beams (Harries and Shahrooz, 2005 and Harries et al. 2000).

3. Based on the established coupling beam design, determine the forces in and design the wall piers. Use an elastic analysis to model the desired coupling "frame" action. From this model, determine the loading effects of the coupling on the wall piers.
4. Use a non-linear analysis to develop axial load-moment-curvature relationships for the beams and the walls.
5. Perform a complete non-linear "pushover" analysis that will determine the displacements of the CCW structure, and compare to the established Target Building Performance Levels.

Harries et al. (2004b) and Harries and McNeice (2006) provide examples of 10 and 30 story CCW designs, respectively, carried out using the proposed PDB methodology. In both cases, structures that may not be "designable" using SBD methods are easily designed and shown to perform very well.

2.1.4 Dynamic Behavior of Coupled Systems

As mentioned earlier, the behavior of CCW structures make these structures especially attractive in earthquake-resistant construction. The desired behavior of CCWs results in the coupling beams serving to dissipate energy over the entire height of the structure. Therefore, it is important to consider the damping and stiffness properties of the beam when completing a design. Depending on the degree of coupling, the beams help reduce story level wall rotations and deflections, which greatly reduces the magnitude of the oscillations that an un-coupled wall structure would otherwise experience. Additionally, developing interaction between wall piers having different dynamic properties can result in improved behavior over the individual systems and over that of the sum of individual systems.

The effects of coupling two structures having different dynamic characteristics can be seen from the results of a study reported by Minami et al. (2004). In this study, two SDOF portal frame structures were assembled each consisting of single large masses supported on four columns as shown in Figure 2.2. Several mass and stiffness combinations were modeled. The structures were connected at the mass level by a vertically oriented steel plate, with one structure fixed at either end of the plate. By careful selection of the plate dimensions (stiffness), different

hysteretic damping properties were achieved. The structure was then tested on a shaking table, which was programmed with scaled seismic ground motion records from the 1940 El Centro (NS component) and the 1995 JMA-Kobe (NS) earthquakes.

Different relationships between the structures were tested, including the ratio of natural periods of the SDOF portal frames as defined by their respective stiffnesses and masses. The results of this experimental study were clear: the coupling of two structural components greatly reduces the deflections in the time history plots of the structures. Additionally, and most importantly, the degree of deflection control may be optimized based on structural and dynamic properties of the system. When coupled, the structures share stiffness and interact with each other, resulting in a greater benefit than if they were simply to behave as the sum of their components. It can be seen in Figure 2.3 (showing El Centro response) that although the initial displacements are similar to the un-coupled response, the oscillations of the structures as time advances diminishes to smaller levels. This behavior results in a much smaller distance traveled by each story level for the same period of time, reducing apparent accelerations and expected structural damage. The shaking experienced by the structure is less intense and therefore also less detrimental to the post-earthquake condition of the building.

The experiment described is applicable to CCW structures, as each structure may represent one wall. In this representation, a combination of coupling beam properties for a given wall layout (geometry and properties) may be optimized to provide a significantly improved response to earthquake ground motion. In the more complex problem, the wall properties ***and*** beam properties may be theoretically optimized to minimize seismic effects. The Minami experiment linked two single degree of freedom (SDOF) structures to simplify the dynamic analysis. This concept will be used in the parametric study (Chapter 3) to study the optimization of coupling beams for given combinations of wall piers, thus demonstrating the parallel of this experiment to CCW structures.

2.2 DERIVATION OF EQUIVALENT SDOF SYSTEM

The first step to modeling a structure is to simplify it to a level that can easily be analyzed. For the present study, it is required to model multi-degree of freedom (MDOF) wall piers as

equivalent single degree of freedom (SDOF) idealizations. When modeled as an equivalent SDOF system, the wall piers of the structure are represented by beam-column members that do not have mass, but have the geometric and mechanical properties (cross sectional area, modulus of elasticity, and moment of inertia) resulting in the column having the appropriate equivalent SDOF stiffness. The equivalent SDOF mass is lumped at the top of these beam-columns resulting in an idealized inverted pendulum.

The equivalent SDOF system may be defined in a variety of ways. For the application that is the subject of this work, it is desired to obtain an equivalent SDOF mass for the original MDOF system. In order to investigate the effects of coupling the MDOF system, it is necessary to locate the equivalent SDOF mass at a particular location of interest. In this study, the equivalent SDOF mass will be located at the roof level of the original MDOF structure. For other applications – for instance the optimization of an outrigger structure located at another discrete point along the structure's height – it may be desired to assess the equivalent SDOF mass at another location. Once the equivalent SDOF mass is determined, the equivalent SDOF stiffness is calculated. Seto et al. (1987) present a simple "eigenvector method" of generically establishing the equivalent SDOF mass at any DOF of an MDOF system. This method is outlined below.

The eigenvector method starts with a known MDOF system. The symmetric stiffness matrix is assembled in the conventional manner and takes the form:

$$\mathbf{K} = \begin{bmatrix} k_{11} & k_{12} & \dots & k_{1j} \\ k_{21} & k_{22} & & \\ \dots & & \dots & \\ k_{j1} & & & k_{jj} \end{bmatrix} \tag{2.2}$$

Where k_{ij} is the stiffness coefficient equal to the restoring force generated at DOF i due to a unit displacement at DOF j, while holding all other DOF's fixed. For a cantilever wall MDOF assumed to have a single DOF located at each floor, **K** is a symmetric matrix having entries only on the main diagonal and in the locations immediate adjacent the main diagonal. All other entries are zero. Additionally, if the wall is modeled as a single uniform flexural element, the lateral stiffness associated with each story is:

$$k = \frac{12EI}{h^3} \tag{2.3}$$

where E and I are the wall modulus and moment of inertia, respectively and h is the story height. The lateral stiffness may be adjusted to account for the presence of shear if required, although this is not done in the present study. Therefore for the case of a uniform cantilever wall the stiffness matrix becomes (DOFs numbered from 1 at 1st floor and increase to roof in this case):

$$\mathbf{K} = \begin{bmatrix} 2k & -k & 0 & \dots & 0 \\ -k & 2k & -k & & \\ 0 & -k & 2k & & \\ \dots & & & \dots & -k \\ 0 & & 0 & -k & k \end{bmatrix} \tag{2.4}$$

For an MDOF cantilever wall pier, masses are lumped at each story and represent the entire story mass tributary to the wall (m_j). The diagonal mass matrix is thus:

$$\mathbf{M} = \begin{bmatrix} m_1 & 0 & \dots & 0 \\ 0 & m_2 & & \\ \dots & & \dots & \\ 0 & & & m_j \end{bmatrix} \tag{2.5}$$

The importance of finding the mass and stiffness matrices lies in the application of D'Alembert's principle of dynamic equilibrium. This principle is founded on Newton's second law of motion: for a constant mass, the force applied to a system is equal to the product of the mass and the acceleration of the mass (Tedesco, 1999). The corresponding equation of motion can be written as:

$$\mathbf{M} \cdot \ddot{x} + \mathbf{C} \cdot \dot{x} + \mathbf{K} \cdot x = \mathbf{F}(t) \tag{2.6}$$

where **F**(t) is the dynamic forcing function and x is the resulting displacement as a function of time (x(t)). Thus $\dot{x}$ is the system velocity and $\ddot{x}$ is the system acceleration. **F** and x are column vectors with entries corresponding to the response at each DOF. When no force is applied, and no damping is provided, equation 2.5 can be re-written as:

$$\mathbf{M} \cdot \ddot{x} + \mathbf{K} \cdot x = \mathbf{0} \tag{2.7}$$

Assuming a general free vibration response, the displacement vector is written as:

$$x(t) = \phi_n (A_n \cos \omega_n t + B_n \sin \omega_n t)) \tag{2.8}$$

Where ω_n is the modal frequency of the structure and φ_n is column vector representing the corresponding mode shape. Substituting equation 2.8 into 2.7 and rearranging terms results in:

$$\left(-\omega_n^2 \mathbf{M}\phi_n + \mathbf{K}\phi_n\right)(A_n \cos \omega_n t + B_n \sin \omega_n t) = \mathbf{0} \tag{2.9}$$

Neglecting the right-hand term in Equation 2.9 which, when equal to zero represents a trivial solution, Equation 2.9 may be rewritten:

$$\left(\mathbf{K} - \omega_n^2 \mathbf{M}\right)\phi_n = \mathbf{0} \tag{2.10}$$

Again, setting $\varphi_n = 0$ represents a trivial solution. The useful solution results by solving the eigenvalue problem represented by:

$$\left|\mathbf{K} - \omega_n^2 \mathbf{M}\right| = 0 \tag{2.11}$$

The roots of equation 2.11 are the system eigenvalues. The eigenvalues, ω_n^2, are then substituted back into equation 2.10 to determine the eigenvectors, φ_n. By substituting all of the eigenvalues into equation 2.10, all eigenvectors are found, and when they are combined together, they form the modal matrix (Tedesco, 1999). The eigenvectors in the modal matrix represent the normal modes of vibration for the structure. Typically, the behavior of relatively uniform building structures is dominated by their first vibration mode shape.

The general eigenvectors are normalized by the value corresponding to the DOF of interest. In most structural applications, the eigenvectors are normalized by a control DOF – typically the roof DOF – or by the maximum value in the eigenvector. The normalization, however, may be against any DOF of interest (Seto, 1987). In the present work, the normalization is made using the roof DOF. Thus the normalized eigenvectors become:

$$\phi_n = \begin{Bmatrix} x_{roof} / x_{roof} \\ \cdots \\ x_n / x_{roof} \\ \cdots \\ x_2 / x_{roof} \\ x_1 / x_{roof} \end{Bmatrix} \tag{2.12}$$

In equation 2.12, the subscript values refer to the DOF or story number (hence 1 is at the bottom).

The equivalent mass of the equivalent SDOF system corresponding to each fundamental mode is found as the product of the transpose of the normalized eigenvector with the mass matrix and the normalized eigenvector (Seto, 1987):

$$M_n = \phi_n^T \mathbf{M} \phi_n \tag{2.13}$$

Finally, the equivalent SDOF stiffness is determined by substituting M_n and the eigenvalue ω_n^2 into equation 2.10:

$$K_n = M_n \omega_n^2 \tag{2.14}$$

To write the eigenvalues in a form having a physical meaning for the structure, the frequency (in Hz) is determined as: $\omega_n / 2\pi$ and the period as: $T = 2\pi / \omega_n$.

For the present study, only the fundamental natural frequency is considered, thus only the first mode shape is used and n =1 throughout the preceding equations. These calculated dynamic properties constitute the relevant components of the equivalent SDOF system corresponding to the roof DOF. As alluded to above, when two parallel walls are to be connected as a coupled core wall system, it is desirable to simplify each wall to its own equivalent SDOF system. Once this operation has been carried out, the next step of finding an optimal, yet practical, coupling system (stiffness and damping) can be pursued using Fixed Point Theory.

2.3 FIXED POINT THEORY

Fixed Point Theory (also know as the Theory of P,Q) is used to optimize interaction stiffness and damping properties of two structures that are in close proximity to each other (Iwanami et al., 1996). Traditionally, this method is used to optimize damping properties for problems of dynamic isolation. In such an application, the two structures considered are the supporting structure (floor or entire building) and the structure to be isolated (often machinery). The two structures typically have exceptionally different dynamic properties in this case. The objective of applying fixed point theory in such a case is to determine the required damping to minimize transmissibility of vibrations between structures. Other applications include optimizing passive damping systems for structural control where the damping system is placed between two components of the structure (such as dampers for cable stays). In most applications, the stiffness of the damping system is negligible. Iwanami et al. (1996) however demonstrate that fixed point theory may be used to determine an optimal combination of damping and stiffness. This approach is applied in the present work.

The premise of the current work is that coupling beams in CCWs provide both stiffness and damping and therefore affect the transmissibility of ground motions through coupled wall piers. The individual wall piers, in this case, represent the two structures for which fixed point theory is applied to determine optimal coupling beam stiffness and damping properties. The specific application will be discussed further in Chapter 3.

2.3.1 Transmissibility

Transmissibility in the present context is defined simply as the ratio of structural lateral deflection to that of the input horizontal ground motion:

$$T = \delta_{structure} \big/ \delta_{ground\ motion} \tag{2.15}$$

In the present work, only unidirectional horizontal ground motion is considered. With the exception of extremely stiff building structures (single story masonry, for instance), T > 1. This indicates that ground motion is amplified by the structure. Thus a valid performance objective is to minimize this transmissibility.

2.3.2 Fixed Point Theory

In this work the following idealized model is considered: two wall piers modeled as equivalent SDOF systems connected to each other with damping and spring elements. The connecting elements allow the pier stiffnesses to help each other decrease transmissibility of the overall structure due to movement induced by a horizontal ground motion. The transmissibility is reliant upon the stiffness and damping values of the connecting elements. These elements can be optimized for a given pair of equivalent SDOF structures. This system is shown schematically as a 2DOF system in Figure 2.4. The system consists of two SDOF systems linked at the top with a dashpot and spring in parallel.

D'Alembert's principle of dynamic equilibrium is applied to determine the following equations of motion for each mass (Iwanami et al., 1996).

$$m_1 \cdot \ddot{x}_1 = k_1 \cdot (u - x_1) + k \cdot (x_2 - x_1) + c \cdot (\dot{x}_2 - \dot{x}_1) \tag{2.16}$$

$$m_2 \cdot \ddot{x}_2 = k_2 \cdot (u - x_2) + k \cdot (x_1 - x_2) + c \cdot (\dot{x}_1 - \dot{x}_2) \tag{2.17}$$

In equations 2.16 and 2.17, u is the ground displacement, k is the spring stiffness, and c is the dashpot damping. Values with subscripts refer to properties of wall piers 1 and 2 as shown in Figure 2.4. If the system is subject to harmonic vibration, two equations can be developed for the transmissibility of the two masses. Transmissibility is the ratio of the displacement at the top of the structure, x(t), to the displacement at the base of the structure: the input ground motion, u(t). These equations were derived by Iwanami et al. (1996), and are functions of the structures' masses and stiffnesses, as well as the spring stiffness, dashpot damping, and natural frequency of the input vibration:

$$\left|\frac{x_1}{u}\right| = \sqrt{\frac{\left[1-\left[\frac{\omega}{\omega_2}\right]^2+\left(\frac{\omega_1}{\omega_2}\right)^2\left(\frac{\eta}{\mu}\right)+\eta\right]^2+\left[2\xi\left(\frac{\omega}{\omega_2}\right)\left[1+\mu\left(\frac{\omega_2}{\omega_1}\right)^2\right]\right]^2}{\left[\left[1+\eta-\left(\frac{\omega}{\omega_1}\right)^2\right]\left[1-\left(\frac{\omega}{\omega_2}\right)^2\right]+\left(\frac{\eta}{\mu}\right)\left[\left(\frac{\omega_1}{\omega_2}\right)^2-\left(\frac{\omega}{\omega_2}\right)\right]\right]^2+\left[2\xi\left(\frac{\omega}{\omega_2}\right)\left[1+\mu\left(\frac{\omega_2}{\omega_1}\right)^2-(1-\mu)\left(\frac{\omega}{\omega_1}\right)^2\right]\right]^2}} \tag{2.18}$$

$$\left|\frac{x_2}{u}\right| = \sqrt{\frac{\left[1-\left[\frac{\omega}{\omega_1}\right]^2+\left(\frac{\omega_1}{\omega_2}\right)^2\left(\frac{\eta}{\mu}\right)+\eta\right]^2+\left[2\xi\left(\frac{\omega}{\omega_2}\right)\left[1+\mu\left(\frac{\omega_2}{\omega_1}\right)^2\right]\right]^2}{\left[\left[1+\eta-\left(\frac{\omega}{\omega_1}\right)^2\right]\left[1-\left(\frac{\omega}{\omega_2}\right)^2\right]+\left(\frac{\eta}{\mu}\right)\left[\left(\frac{\omega_1}{\omega_2}\right)^2-\left(\frac{\omega}{\omega_2}\right)\right]\right]^2+\left[2\xi\left(\frac{\omega}{\omega_2}\right)\left[1+\mu\left(\frac{\omega_2}{\omega_1}\right)^2-(1-\mu)\left(\frac{\omega}{\omega_1}\right)^2\right]\right]^2}} \tag{2.19}$$

Where: ω = frequency of the forcing function;

ω_i = frequency of wall pier i = 1 or i = 2: $\omega_i = \sqrt{k_i/m_i}$;

η = the ratio of the spring stiffness to the stiffness of wall 1 (also known as the fixed point stiffness ratio): $\eta = k/k_1$;

μ = the mass ratio of the wall piers: $\mu = m_2/m_1$; and,

ξ = damping ratio: $\xi = c/2\sqrt{m_2 k_2}$

When the transmissibility equations for each wall are alternately expressed with damping (ξ) equal to zero and ξ equal to infinity, the results are three curves as shown schematically in Figure 2.5. When $\xi = \infty$, the connecting element becomes essentially rigid, creating a SDOF system in which the masses displace by the same amount, and thus the transmissibility of each wall is equal. The curves shown in Figure 2.5 have six intersection points. The two points of

wall is equal. The curves shown in Figure 2.5 have six intersection points. The two points of interest, labeled "P" and "Q", are shown in Figure 2.5. These interstices are those that correspond to the physical reality that when $\xi = \infty$, the transmissibility of each wall must be equal.

When the equations given by 2.18 and 2.19 for the transmissibility of each wall pier are plotted on the same graph, it is apparent that their maximum values correspond to points P and Q, respectively (see Figure 2.5). As shown in Figure 2.6, after manipulation of the ratios η, μ, and γ, it is observed that the maximum transmissibility values always occurs near points P and Q, and that these values are different depending on the aforementioned ratios (Iwanami et al., 1996). The necessary interaction between parameters in order to optimize the problem is also demonstrated in Figure 2.6.

The optimum transmissibility of the system is achieved when the transmissibility values of P and Q are equal (i.e.: when plotted, they fall on the same horizontal line in the plot). The optimum values of η and ξ are found through trial and error by selecting values for μ and γ, and plotting the transmissibility equations to determine how close the transmissibility values at P and Q are to equality. The ratios are varied until the transmissibility values at P and Q are nearly equal, meaning the system is optimized. Iwanami et al. (1996) suggest that this optimization is achieved when the transmissibility values are within 3% of each other. This represents the optimum set of ratios of mass, natural frequency, stiffening, and damping for the system.

It is desirable to bypass this trial and error approach for a more efficient solution of the problem through the use of a closed form solution. A closed form solution is also practical in the case of the CCW problem considered, since the ratios μ and γ are defined by the problem and may not be varied, resulting in a solution having only two unknowns: η and ξ. It will be further proposed in subsequent chapters that a structural engineering problem such as a CCW likely has a very narrow practical range of values for the damping coefficient, ξ, and a broader (although still limited) range of practical values for the coupling beam stiffness, k. Thus the problem may not be truly optimized, but optimized based on a set of fixed input values. In such a case a closed form solution is practical.

Such a closed from solution has been proposed by Richardson (2003). In this approach, the fixed point stiffness ratio, η, is found, followed by the damping values associated with points P and Q (ξA and ξB respectively). The optimized damping ratio is taken as the average of these

damping values. Critical aspects of the closed form solution are presented through its use in Chapter 3. The complete closed form solution (in MathCad format) is presented in Appendix A in support of the parametric study described in Chapter 3. It is critical to note that in the application of the closed form solution the wall designations (1 and 2) must be selected such that $\omega_2/\omega_1 > 1.0$.

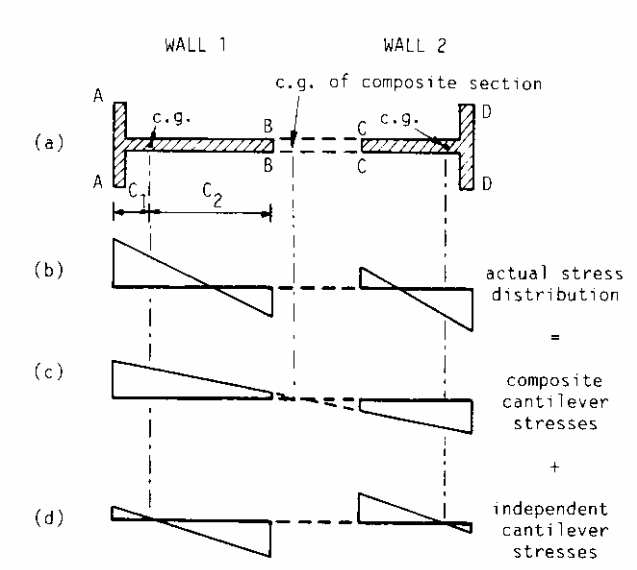

Figure 2.1 Distribution of wall pier forces for coupled and uncoupled structures (Stafford-Smith and Coull, 1991)

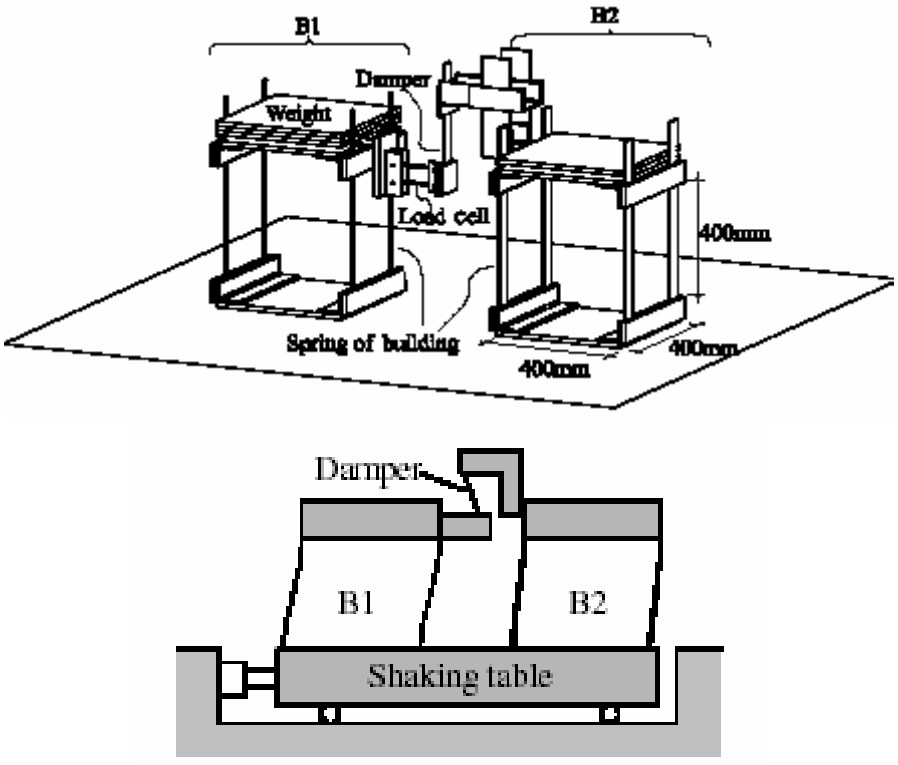

Figure 2.2 Coupled SDOF structures and two-dimensional idealization (Minami et al, 2004)

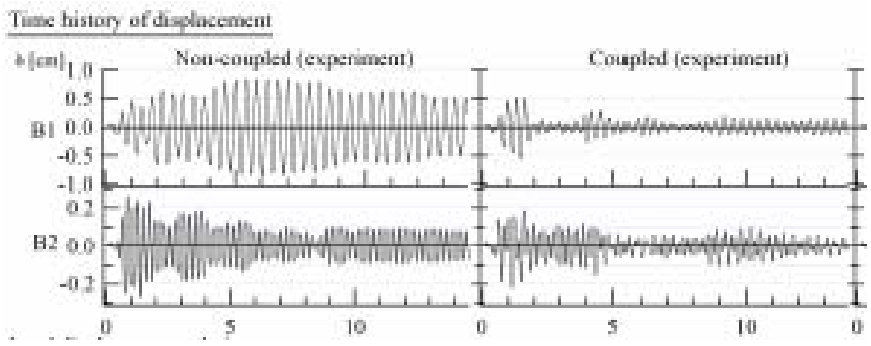

Figure 2.3 Effect of coupling on deflection time histories of coupled SDOF structures (Minami et al, 2004)

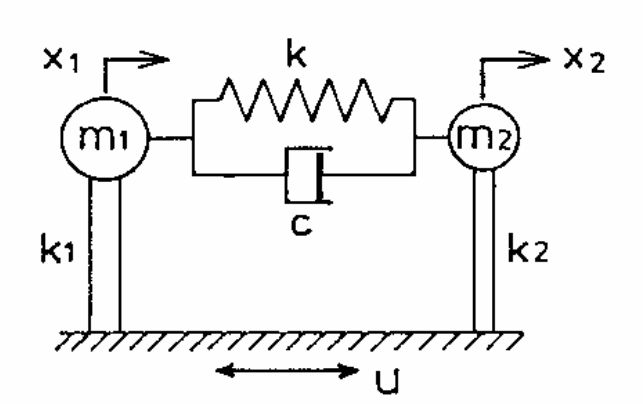

Figure 2.4 Idealized 2DOF system for application of Fixed Point Theory (Iwanami et al, 1996)

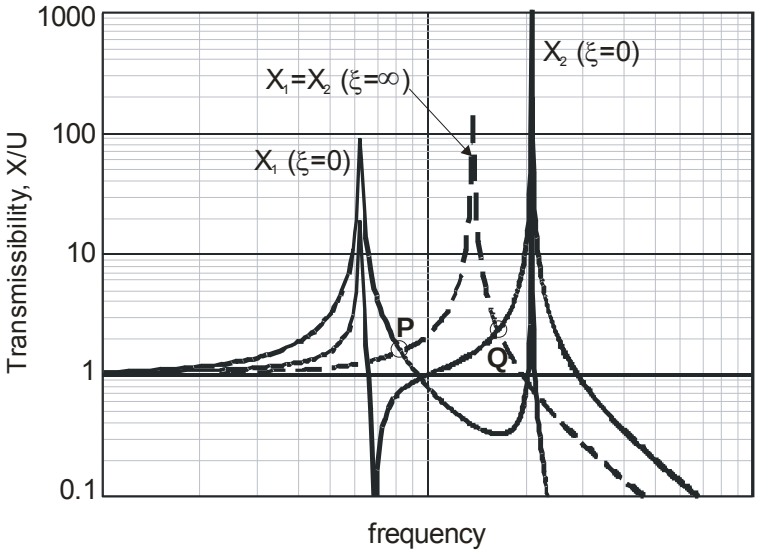

Figure 2.5 Schematic representation of transmissibility vs. structural frequency curves (after Iwanami et al., 1996).

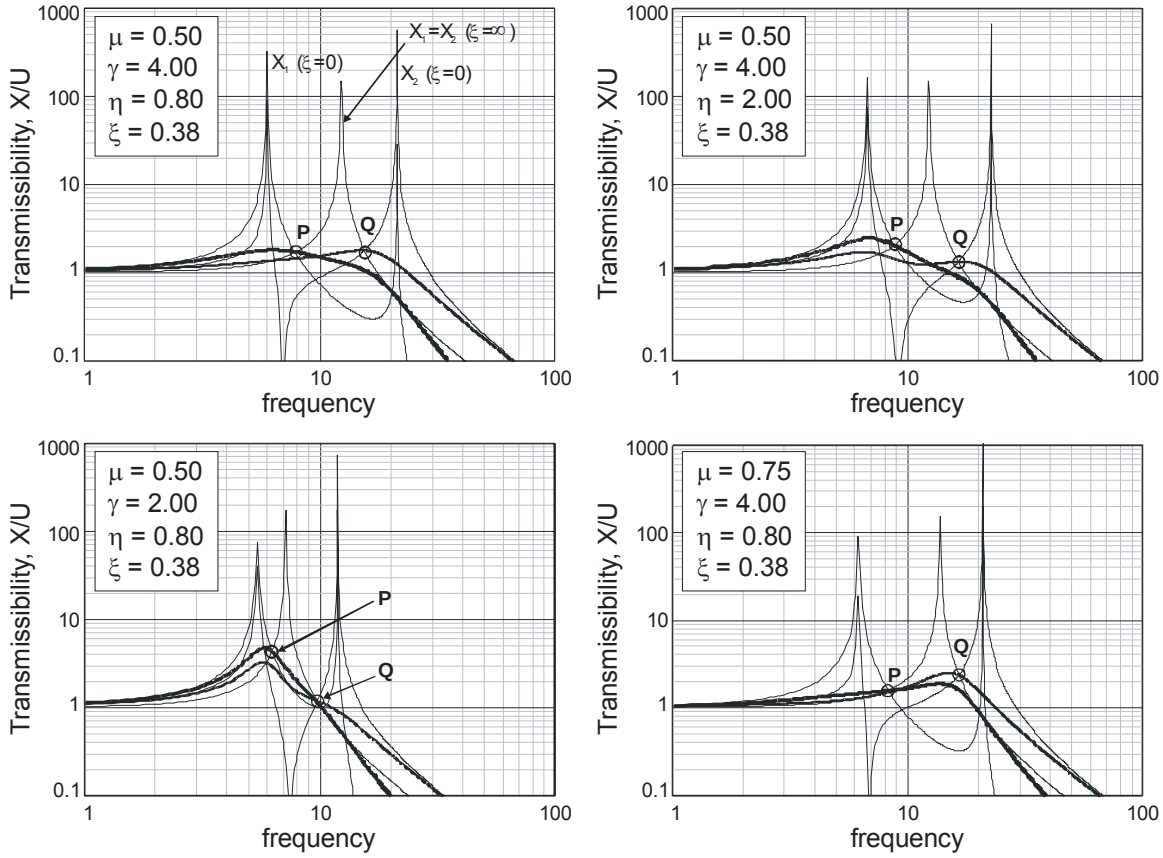

Figure 2.6 Effect of varying μ, η, and γ on transmissibility curves.
Upper left plot is only plot having optimized values (after Iwanami et al., 1996)

3.0 PARAMETRIC APPLICATION OF FIXED POINT THEORY

The objective of this work is to present a preliminary exploration of the use of Fixed Point Theory as a means of optimizing coupled core wall (CCW) behavior. As described in Chapter 2, simplified closed form solutions will be undertaken requiring a number of generalizations. Additionally, it is not suggested in this work that the coupled wall geometries presented are representative of viable building geometries; they are however based on geometries used in a previous parametric study of CCW behavior (Harries et al. 2004a).

In previous analytical studies, the individual wall piers of a CCW system are assumed to have the same geometry. This simplifies analysis and renders the optimization of transmissibility represented by the fixed point approach trivial since both walls piers have the same dynamic properties to begin with. The methodology examined in the present work require individual wall piers of a CCW to have different dynamic properties.

3.1 PROTOTYPE STRUCTURES

Prototype structures having wall pier geometries previously identified by Harries et al (2004a) are used. Seven pier geometries (labeled A through G) are used – these are shown schematically in Figure 3.1 and the dimensions used are presented in Table 3.1. In all cases, wall thickness is assumed to be uniform at 0.760 m. The individual wall piers are paired into two pier CCWs – each pier matched with each different pier – resulting in 21 analyses for each case (see below). Again, it is noted that matching a wall pier with itself (A-A, say) results in a trivial case as far as the optimization of transmissibility is concerned. An example of matched wall piers D-E is shown in Figure 3.2. The coupling beam length and cross sectional dimensions are not relevant at this stage in the study as only the dynamic properties of the individual piers are considered.

Wall dimensions are provided largely to lend credibility to the selection of dynamic properties for the parametric study. Only two-dimensional loading in the coupled direction (left-to-right in Figure 3.2) is considered in this preliminary study; thus torsional effects and uncoupled wall behavior in the transverse direction are not considered.

In the initial parametric study, four cases are considered involving two building heights and the use of uncracked and cracked section properties. Details of the cases are provided in Table 3.2. Twelve (cases 1 and 3) and twenty-four story (cases 2 and 4) versions of each CCW arrangement are considered. Story heights are maintained constant in all cases at 3.60 m. One set of cases (1 and 2) uses the wall piers' gross section properties, EI_g, throughout the height of the structure. Cracked section properties recommended by clause 10.11.1 of ACI 318 (2005) are used in cases 3 and 4. The cracked section properties assume a flexural stiffness of $0.35EI_g$ in the lower floors corresponding to the expected hinging region - 2 stories in the 12 story structure and 3 stories in the 24 story structure – and $0.70EI_g$ throughout the remainder of the height. These cracked section properties are consistent with common west coast practice in preliminary CCW sizing and design. The value of E = 28.5 GPa is assumed in all analyses.

In all cases, floor weights are assumed to be 10,000 Mg. These are distributed to the wall piers in proportion to the wall pier area and are thus used in determining the degree of freedom (DOF) masses for each wall pier at each floor

3.2 PARAMETRIC ANALYSIS

The parametric analysis was carried out using an integration of MathCad and Excel worksheets. The complete MathCad worksheet showing the entire procedure discussed below is provided in Appendix A. The following sections follow the step-by-step procedure used to arrive at the optimized transmissibility parameters for each pair of walls in each case. In all, 84 separate analyses were conducted. The results of these are presented in Appendix B. For clarity, the following step-by-step summary includes values determined for twelve story wall piers D and E, each having cracked section properties (Trial #3-16 in Appendix B). The calculation of the optimal conditions for this combination is desirable since it will be used for the linear dynamic time history analysis in Chapter 4. At the beginning of every case, the wall piers are arbitrarily

designated "1" and "2" in the MathCad worksheet. In the third step, these designations are checked and may be reversed to satisfy the requirement that the ratio of wall frequencies, $\omega_2/\omega_1 > 1.0$.

3.2.1 Step 1: Assembling MDOF Model of Each Wall Pier

For Trial #3-16, Wall D is designated as "1" and Wall E is "2". Thus:

A1 = 11.005 m^2 and $I1_g$ = 26.5653 m^4 ; A2 = 7.965 m^2 and $I2_g$ = 6.0291 m^4

The value of E = 28.5 x 10^9 N/m^2. The building is twelve stories high, with story heights of 3.60 m, and the mass at each story level is assumed to be 10,000Mg. The story mass is apportioned to each wall as the ratio of the wall areas. Thus the DOF masses of each wall become:

$$m_x = \frac{A_x}{A1 + A2} \cdot m_{Total} \text{ for x representing walls 1 and 2.} \quad (3.1)$$

The values of m1 and m2 are thus found to be 5.801 x 10^6 kg and 4.199 x 10^6 kg, respectively. The 12 x 12 MDOF mass matrices are thus assembled for walls 1 and 2:

$$\mathbf{M}x = \begin{bmatrix} mx & 0 & \dots & 0 \\ 0 & mx & & \\ \dots & & \dots & \\ 0 & & & mx \end{bmatrix} \text{ for x representing walls 1 and 2.}$$

The lateral stiffness of each story is given as:

$$k_x = \frac{12EI_x}{h^3} \text{ for x representing walls 1 and 2.} \quad (3.2)$$

The values of k1 and k2 are thus found to be 1.947 x 10^{11} N/m and 4.419 x 10^{10} N/m, respectively. The 12 x 12 MDOF stiffness matrices are thus assembled for walls 1 and 2:

$$\mathbf{K}x = \begin{bmatrix} 0.70kx & -0.35kx & 0 & 0 & \dots & 0 \\ -0.35kx & 1.05kx & -0.70kx & 0 & \dots & 0 \\ 0 & -0.70kx & 1.40kx & -0.70kx & \dots & 0 \\ 0 & 0 & -0.70kx & 1.40kx & \dots & \dots \\ \dots & \dots & \dots & \dots & \dots & -0.70kx \\ 0 & 0 & 0 & \dots & -0.70kx & 1.40kx \end{bmatrix}$$

with x representing walls 1 and 2.

The coefficients 0.35 and 0.70 in the stiffness matrix correspond to the cracked material properties. In these formulations, DOF 1 is the first floor lateral deflection and DOF 12 is the roof lateral deflection of the 12 DOF cantilever column representation of the wall pier.

3.2.2 Step 2: Generate Equivalent SDOF of each wall pier

Each 12 DOF cantilever wall is reduced to an equivalent SDOF system as described in Chapter 2 by solving the eigenvalue problem represented in Equation 2.10:

$$\left(\mathbf{K} - \omega_n^2 \mathbf{M}\right)\phi_n = \mathbf{0} \tag{3.3}$$

The lowest or fundamental eigenvalue, ω^2, is of interest in generating the equivalent SDOF system. For wall 1, the fundamental eigenvalue, $\omega_1^2 = 279.75$. From this value, the fundamental or first mode eigenvector, φ_1, is found and normalized by the DOF of interest; in this case the roof DOF (DOF 12). The normalized fundamental eigenvector for wall 1 is thus determined to be:

$$\phi 1_1 = \begin{Bmatrix} DOF1 \\ DOF2 \\ \dots \\ \\ \\ \\ \\ \\ \\ \\ \dots \\ DOF12 \end{Bmatrix} = \begin{Bmatrix} 0.209 \\ 0.413 \\ 0.509 \\ 0.600 \\ 0.684 \\ 0.760 \\ 0.826 \\ 0.883 \\ 0.929 \\ 0.964 \\ 0.988 \\ 1.000 \end{Bmatrix} \tag{3.4}$$

From the eigenvector (Equation 3.4), the equivalent SDOF mass (or modal mass) is determined as:

$$em1 = \left\{\phi 1_1^T\right\}\mathbf{M1}\left\{\phi 1_1\right\} = 4.126x10^7 \ \ kg \tag{3.5a}$$

Similarly, for wall 2:

$$em2 = \{\phi 2_1^T\}\mathbf{M2}\{\phi 2_1\} = 2.986x10^7 \ \ kg \tag{3.5b}$$

The natural frequency of each wall pier is calculated from the eigenvalues:

$$\omega_1 = \sqrt{\omega_1^2} = \sqrt{279.75} = 16.726 \ \ radians/\sec \text{; and,} \tag{3.6a}$$

$$\omega_2 = \sqrt{\omega_2^2} = 9.366 \ \ radians/\sec \tag{3.6b}$$

The final step of developing a SDOF system from an MDOF system is to calculate the equivalent SDOF stiffness for both walls:

$$ek1 = (em1)\omega_1^2 = 1.154x10^{10} \ \ N/m \text{; and,} \tag{3.7a}$$

$$ek2 = (em2)\omega_2^2 = 2.619x10^9 \ \ N/m \tag{3.7b}$$

Thus the equivalent SDOF systems having equivalent mass, em, and equivalent stiffness, ek, are determined. Using these SDOF systems, fixed point theory is applied to optimize transmissibility.

3.2.3 Step 3: Apply Closed Form Solutions to Fixed Point Theory

The closed form solution for optimization of transmissibility developed by Richardson (2003) requires that $\omega_1 < \omega_2$. This step is included in the MathCad worksheet presented in Appendix A. Thus in the example developed above, the designations of wall 1 and wall 2 must be reversed; therefore from this step onward:

Wall E is wall 1 and wall D is wall 2;

$\omega_1 = 9.366$ rad/s and $\omega_2 = 16.726$ rad/s;

em1 = 2.986 x 10^7 kg and em2 = 4.126 x 10^7 kg; and,

ek1 = 2.619 x 10^9 N/m and ek2 = 1.154 x 10^{10} N/m.

The solution continues establishing the ratios between fundamental properties of the individual SDOF systems:

mass ratio = μ = em2/em1 = 1.382 (3.8)

frequency ratio = $\gamma = \omega_2/\omega_1 = 1.786$ (≥ 1.0) (3.9)

The fixed point stiffness ratio, η = k/ek1, where k is the optimized coupling beam stiffness, remains to be determined. The fixed point stiffness ratio may be determined as:

$$\eta = U/L \tag{3.10}$$

where,

$$U = \frac{1}{4}\cdot(-\omega_1+\omega_2)\cdot(\omega_1+\omega_2)\cdot(-3\cdot(\mu+5)\cdot(\mu+1)^2\cdot\omega_1^{\,6}-3\omega_2^{\,2}\cdot(7\mu+3)\cdot(\mu+1)^2\cdot\omega_1^{\,4}$$
$$+\left[\left(3\mu^5+15\mu^2+33\mu^3+21\mu^4\right)\cdot\omega_2^{\,4}-3\sqrt{g}+\mu\sqrt{g}\right]\cdot\omega_1^{\,2}+$$
$$(21\mu^5+51\mu^4+39\mu^3+9\mu^2)\cdot\omega_2^{\,6}+(3\mu^2\sqrt{g}-\mu\sqrt{g})\cdot\omega_2^{\,2})\cdot\mu \tag{3.11}$$

$$L=(\omega_1^{\,2}\cdot(\mu+1)^2\cdot(\omega_2^{\,2}\mu+\omega_1^{\,2})\cdot[(6\mu+\mu^2+5)\omega_1^{\,4}+13\mu^2+3+\mu^3+15\mu)\omega_2^{\,2}\omega_1^{\,2}$$
$$+(7\mu^3+3\mu+10\mu^2)\omega_2^{\,4}+\sqrt{g})] \tag{3.12}$$

and

$$g=(\omega_2^{\,2}\mu+\omega_1^{\,2})\cdot(\mu^3\omega_2^{\,2}+26\mu^2\omega_2^{\,2}+9\mu^2\omega_1^{\,2}+9\omega_2^{\,2}\mu+26\omega_1^{\,2}\mu+\omega_1^{\,2})\cdot$$
$$(5\omega_1^{\,2}+3\omega_2^{\,2}+\omega_1^{\,2}\mu+7\omega_2^{\,2}\mu)^2 \tag{3.13}$$

For the example case, substituting all the variables into these equations yields:

$U = 1.619 \times 10^{12}$; $L = 4.283 \times 10^{12}$; and, $g = 1.826 \times 10^{14}$

Thus $\eta = U/L = 0.378$.

Next, the frequencies corresponding to the points P and Q, ω_P and ω_Q respectively, are determined:

$$\omega_P=\frac{1}{2}\frac{\sqrt{2}\cdot\sqrt{\mu\cdot(\omega_1^{\,2}\mu+\omega_2^{\,2}\mu+2\omega_1^{\,2})\cdot\omega_{PA}}}{\mu\cdot(\omega_1^{\,2}\mu+\omega_2^{\,2}\mu+2\omega_1^{\,2})} \tag{3.14}$$

where,

$$\omega_{PA}=[(3+2\eta)\omega_2^{\,2}\omega_1^{\,2}+\omega_2^{\,4}]\cdot\mu^2+[(2+2\eta)\omega_1^{\,4}+(2+2\eta)\cdot\omega_2^{\,2}\omega_1^{\,2}]\cdot\mu+2\omega_1^{\,4}\eta-\sqrt{S_P} \tag{3.15}$$

and

$$S_P=4\omega_1^{\,4}\cdot(\mu+1)^2\cdot(\omega_2^{\,2}\mu+\omega_1^{\,2})^2\cdot\eta^2-4\mu\omega_1^{\,2}\cdot(\omega_1-\omega_2)\cdot(\omega_1+\omega_2)\cdot(\omega_2^{\,2}\mu+\omega_1^{\,2})$$
$$(-\mu^2\omega_2^{\,2}+\omega_2^{\,2}\mu+2\omega_1^{\,2})\cdot\eta+\mu^2\cdot(\omega_1-\omega_2)^2\cdot(\omega_1+\omega_2)^2\cdot(2\omega_1^{\,2}+\omega_2^{\,2}\mu)^2 \tag{3.16}$$

Substituting all the variables into equations 3.14 through 3.16 yields:

$S_P = 2.831 \times 10^{10}$; $\omega_{PA} = 2.857 \times 10^{5}$; and, $\omega_P = 12.301$ radians/sec.

Similarly:

$$\omega_Q = \frac{1}{2}\frac{\sqrt{2}\cdot\sqrt{\mu\cdot(2\omega_2{}^2\mu+\omega_2{}^2+\omega_1{}^2)\cdot\omega_{QA}}}{\mu\cdot(2\omega_2{}^2\mu+\omega_2{}^2+\omega_1{}^2)} \tag{3.17}$$

$$\omega_{QA} = [(2+2\eta)\omega_2{}^2\omega_1{}^2+2\omega_2{}^4]\cdot\mu^2+[(1+2\eta)\omega_1{}^4+(3+2\eta)\cdot\omega_2{}^2\omega_1{}^2]\cdot\mu+2\omega_1{}^4\eta+\sqrt{S_Q} \tag{3.18}$$

$$S_Q = 4\omega_1{}^4\cdot(\mu+1)^2\cdot(\omega_2{}^2\mu+\omega_1{}^2)^2\cdot\eta^2-4\mu\omega_1{}^2\cdot(\omega_2-\omega_1)\cdot(\omega_1+\omega_2)\cdot(\omega_2{}^2\mu+\omega_1{}^2)$$
$$(2\mu^2\omega_2{}^2+\omega_1{}^2\mu-\omega_1{}^2)\cdot\eta+\mu^2\cdot(\omega_2-\omega_1)^2\cdot(\omega_1+\omega_2)^2\cdot(2\omega_2{}^2\mu+\omega_1{}^2)^2 \tag{3.19}$$

Substituting all the variables into equations 3.17 through 3.19 yields:

S_Q= 3.938x10^{10}; ω_{QA} = 7.782x10^5; and, ω_Q = 15.714 radians/sec.

The optimal fixed point damping ratio, ξ, is reached when the transmissibility curves are nearly at a maximum at points P and Q, and the transmissibility values of P and Q are nearly equal in magnitude (Iwanami et al. 1996). Mathematically, recalling equations 2.18 and 2.19, the former condition is satisfied when:

$$\frac{dX_1(\omega_P)}{d\omega}=0 \quad \text{and} \quad \frac{dX_2(\omega_Q)}{d\omega}=0 \tag{3.20}$$

Substituting equations 3.14 and 3.17, the solution to equations 3.20 yield two quadratic equations:

$$a_1\xi_1^4+b_1\xi_1^2+c_1=0 \tag{3.21}$$

$$a_2\xi_2^4+b_2\xi_2^2+c_2=0 \tag{3.22}$$

The solutions to equations 3.21 and 3.22 are:

$$\xi_1{}^2=\frac{-b_1\pm\sqrt{b_1{}^2-4a_1c_1}}{2a_1}=0.13 \tag{3.23}$$

and

$$\xi_2{}^2=\frac{-b_2\pm\sqrt{b_2{}^2-4a_2c_2}}{2a_2}=0.12 \tag{3.24}$$

The definitions of the constants a_1, b_1, c_1, a_2, b_2, and c_2 are given in Appendix A. As expected, the damping ratios are very close to being equal. The fixed point damping ratio for the coupling beam is found by taking the average of ξ_1 and ξ_2:

$$\xi = \frac{\xi_1 + \xi_2}{2} = 0.125 \tag{3.25}$$

Finally, the fixed point stiffness is calculated from η as:

$$k = \eta \cdot k1 = 9.901x10^8 \ \ N/m \tag{3.26}$$

Tabulated values of all 21 wall pairs for each of the four cases considered are provided in Appendix B.

3.3 PARAMETRIC STUDY RESULTS

Prior to discussing any results, it is important to note that when the natural frequency ratio, γ, approaches 1.0, ω_1 approaches equality with ω_2. This condition causes equation 3.11 to approach zero, resulting in the calculated fixed point stiffness ratio (equation 3.10) to also approach zero. This represents the trivial case where two identical SDOF systems will have continued identical dynamic behavior (and thus equal transmissibility) regardless of the level of coupling and/or damping provided. Additionally, in the closed form solution, when the product of mass and frequency ratios, μγ, falls below 1.0, the optimization process yields negative stiffness values. Although mathematically correct, such results are not physically meaningful – indicating a negative stiffness is required for optimization. In essence, coupling the wall piers in this case results in increased transmissibility compared to the uncoupled walls. Thus wall combinations with the product of mass ratio to natural frequency ratio at or below 1.0 are neglected in all further discussion. Trial numbers 15 and 19 in all four cases fall into this category, as shown in Appendix B.

The parametric study results show that there is little difference between the four cases considered. Initially, this was troubling but upon further consideration, it is a reflection of the fact that the formulation of fixed point theory relies mostly on ratios of dynamic properties between two equivalent SDOF systems. When the number of floors change for a particular wall combination, the resulting equivalent SDOF mass and stiffness change proportionally; thus the

mass, frequency, fixed point damping, and fixed point stiffness ratios remain essentially unchanged. Similarly, when cracked sections are introduced, the equivalent SDOF stiffness and mass values change, reflecting the lower frequency. However, since both wall piers are considered in the same manner, the resulting ratios, again, remain virtually unchanged. Thus this approach is "normalized" to the ratio between wall pier dynamic properties. This observation may permit eventual generalization of the approach in a manner analogous to spectral analysis methods.

As should be expected, regardless of ratios of properties, numeric values of optimized stiffness and damping are reduced when cracked concrete section properties are used. The resulting reductions are uniform for all structures considered and vary based on the structure height (number of stories) as shown in Table 3.3. The values in Table 3.3 show a more pronounced reduction in optimized properties for the 12 story case. This is a reflection of the proportionally greater (2 of 12 stories; rather than 3 of 24) extent of the assumed hinge region having a cracked stiffness of $0.35EI_g$.

3.4 TWELVE STORY CCW WITH CRACKED WALLS (CASE 3)

Based on the consistency of behavior described above, only the 12 story CCW having cracked section properties will be considered for the remainder of this discussion.

Figures 3.3 and 3.4 show the optimized coupling stiffness and damping ratios, respectively, plotted against the frequency ratios. In order to verify the observed trends at lower frequency ratios than were considered in the database (approaching $\gamma = 1$), six artificial cases were calculated for $\gamma = 1.05$, 1.06, 1.07, 1.08, 1.09, and 1.10. These are indicated with a "Δ" in the figures. It is clear from Figures 3.3 and 3.4 that as the frequency ratio grows – that is: the wall pier dynamic properties are less similar, that the optimized stiffness and damping increases.

In practical applications, there are clearly limits to the damping and/or stiffness that can be developed between wall piers. Thus these plots, and the relationships they represent, give some indication of the "optimizability" of CCW systems. For example, at ultimate load levels, reinforced concrete beams may be expected to provide between 7% and 10% critical damping (Newmark and Hall, 1982). Thus the ability to optimize dynamic behavior would be limited to

walls having relatively similar dynamic properties; having a frequency ratio less than about γ = 1.40. Similarly, the stiffness ratio is given as a ratio of the equivalent SDOF lateral stiffness of wall pier 1. Practical coupling beam stiffness may be assumed to be limited to fractional values of this stiffness. Thus, again a lower bound frequency ratio of for optimization may be assumed (in this case, perhaps γ = 1.65). Although optimization may not be practical outside of a range of parameters, improved transmissibility is still quite viable – the solution is simply not optimized.

3.5 PROTOTYPE STRUCTURE FOR FURTHER STUDY

A single prototype structure is selected for further study: Trial #3-16, matching wall piers D and E and using cracked section properties. The CCW plan for this prototype is shown in Figure 3.2 and the case is highlighted in both Figures 3.3 and 3.4 with a surrounding "□". The dynamic properties determined for this case are as follows:

frequency of wall 1 (E):	ω_1 = 1.491 Hz
frequency of wall 2 (D):	ω_2 = 2.662 Hz
frequency ratio:	γ = 1.79
optimized damping ratio:	ξ = 0.125
optimized stiffness ratio:	η = 0.378

The optimized fixed point curves for this prototype structure are shown in Figure 3.5. The minimized transmissibility for this optimized case is:

Wall 1 (E):	X_1/U = 3.73
Wall 2 (D):	X_2/U = 4.06

The transmissibility of Wall 2 is slightly greater. Wall 2 is the stiffer wall (always the case using this closed form solution since γ > 1.0) and thus experiences proportionally less of a shift from its resonant frequency (the X_2/U (ξ = 0) curve in Figure 3.5) to the point Q than wall 1 does in shifting to point P. This observation is reflected in the following parametric sensitivity analysis.

3.5.1 Effect of damping and stiffness on transmissibility

The damping ratio for the selected prototype, $\xi = 0.125$, is greater than may be practically achieved in a structure without mechanical damping devices. Thus it is instructive to investigate the effect of varying the damping provided on the transmissibility of each wall. Similarly the stiffness ratio may not be optimized or may vary as the structure undergoes seismic excitation. Thus, again it is instructive to vary the stiffness ratio and investigate the effect on transmissibility. Figures 3.6, 3.7 and 3.8 show the transmissibilities determined by varying the damping and stiffness parameters of the prototype structure as follows:

damping: $0.00 < \xi < 0.20$ (calculated at increments of 0.01)

stiffness: $0.00 < \eta < 1.00$ (calculated at increments of 0.05)

Figure 3.6 shows the transmissibility determined for each wall pier, E and D, respectively, for varying damping and stiffness. These values are X_1/U and X_2/U, respectively. Figure 3.8 shows the average transmissibility value for the CCW system. In Figure 3.8, it is clear that the average transmissibility is minimized (average of X_1/U and $X_2/U = 3.9$) at $\xi = 0.125$ and $\eta = 0.378$ as indicated by the +. This point is repeated in Figure 3.6. The optimal transmissibility of each wall pier (Figure 3.6) is a) lower than the optimized value for the CCW system; and b) located at different damping and stiffness ratios. For Wall D the optimal transmissibility is approximately 3.02 and occurs at a damping ratio, $\xi = 0.09$ and essentially zero stiffness. Similarly, the optimal transmissibility for Wall E is also approximately 3.08 and occurs at a damping ratio, $\xi = 0.12$ and a nominal stiffness of $\eta = 0.70$

Figure 3.7 can be used to investigate the sensitivity of the transmissibility to variations in damping and stiffness. It is seen in Figure 3.7, for instance that while the optimal transmissibility is 3.9, the transmissibility remains below 5.0 over most of the range of stiffness values considered for damping values greater than $\xi = 0.08$. Such plots, may be normalized and used as design tools to initiate practical CCW system geometries

Finally, Figure 3.8 shows the transmissibility relationships for the arbitrary, although thought to be structurally feasible, case of $\xi = 0.050$ and $\eta = 0.250$. In this case, the transmissibility becomes:

Wall 1 (E): $X_1/U = 6.30$

Wall 2 (D): $X_2/U = 8.08$

The curves shown in Figure 3.8 clearly indicate that the system is no longer optimized (points P and Q are not correctly determined) and that the behavior of each wall pier is closer to its original resonant condition; that is: the peaks of transmissibility curves lie very close to individual wall pier transmissibility curves ($\xi = 0$), and the peak of each curve no longer corresponds to the fixed points P and Q. As will be shown in Chapter 4, this trade-off between the optimal and the feasible coupling conditions will be further amplified by the linear dynamic analysis.

Table 3.1 Wall combinations for parametric study.

Wall	Wall Length, lw (m)	Wall Width, bw (m)	Gross Wall Area, A (m^2)	Gross Wall Inertia, I (m^4)
A	7.00	9.00	16.325	79.7880
B	6.00	3.00	10.245	34.2875
C	4.00	3.00	7.205	10.6519
D	5.00	6.00	11.005	26.5653
E	3.00	6.00	7.965	6.0291
F	3.00	3.00	5.685	4.6059
G	4.00	9.00	11.765	16.0905

Table 3.2 Effective stiffnesses used for considered cases.

Case	Number of Stories	Effective EI_g *			
		Affected Stories	Reduced Stiffness	Affected Stories	Reduced Stiffness
1	12	1.0 EI_g			
2	24	1.0 EI_g			
3	12	1-2	0.35 EI_g	3-12	0.70 EI_g
4	24	1-3	0.35 EI_g	4-24	0.70 EI_g

*Ref: ACI 318 - 02 Chapter 10.11.1

Table 3.3 Ratio of optimized values determined from cracked sections analysis to those determined for uncracked sections.

# of Stories	Cracked / Uncracked Values	
	Coupling Stiffness	Coupling Damping
12	0.55	0.80
24	0.60	0.82

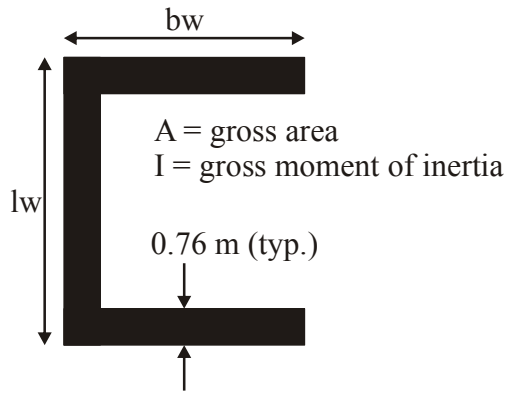

Figure 3.1 Plan of Prototype Wall Pier

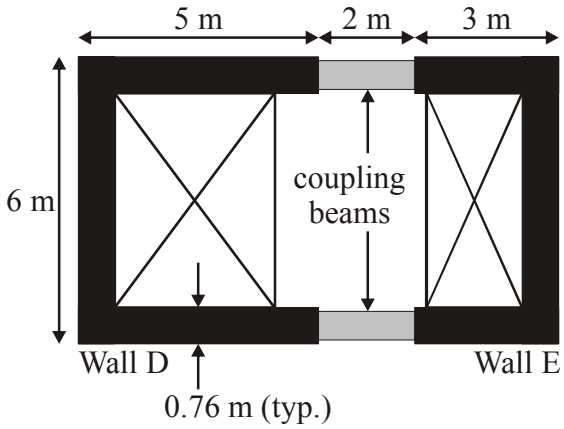

Figure 3.2 Example of Prototype CCW Plan – Walls D and E

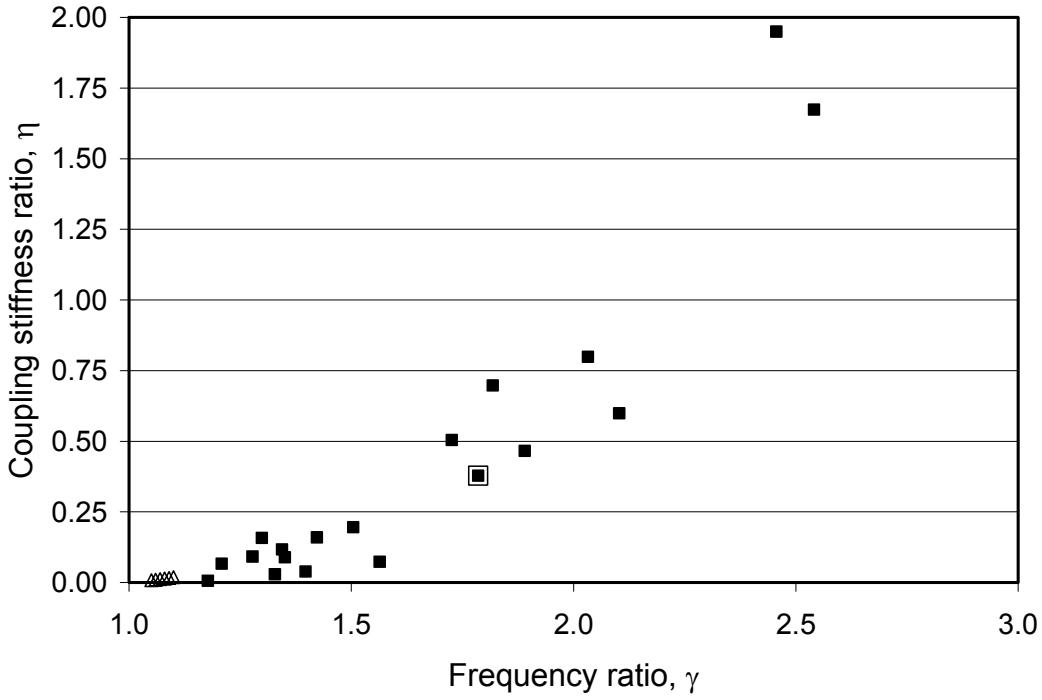

Figure 3.3 Variation of optimized coupling stiffness ratio with frequency ratio.

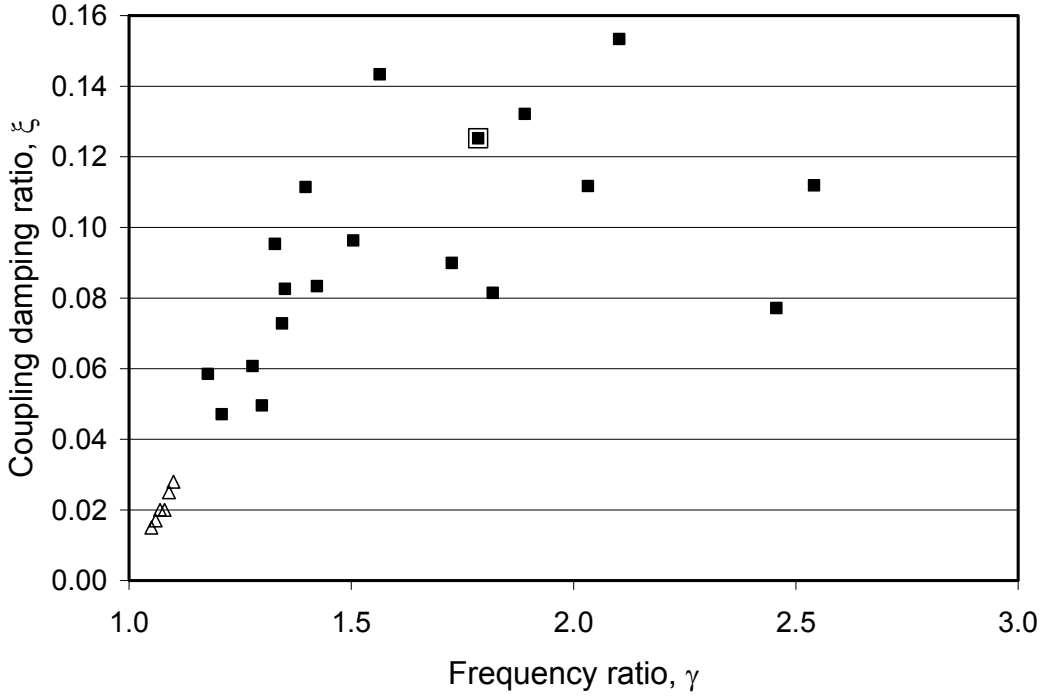

Figure 3.4 Variation of optimized coupling damping ratio with frequency ratio.

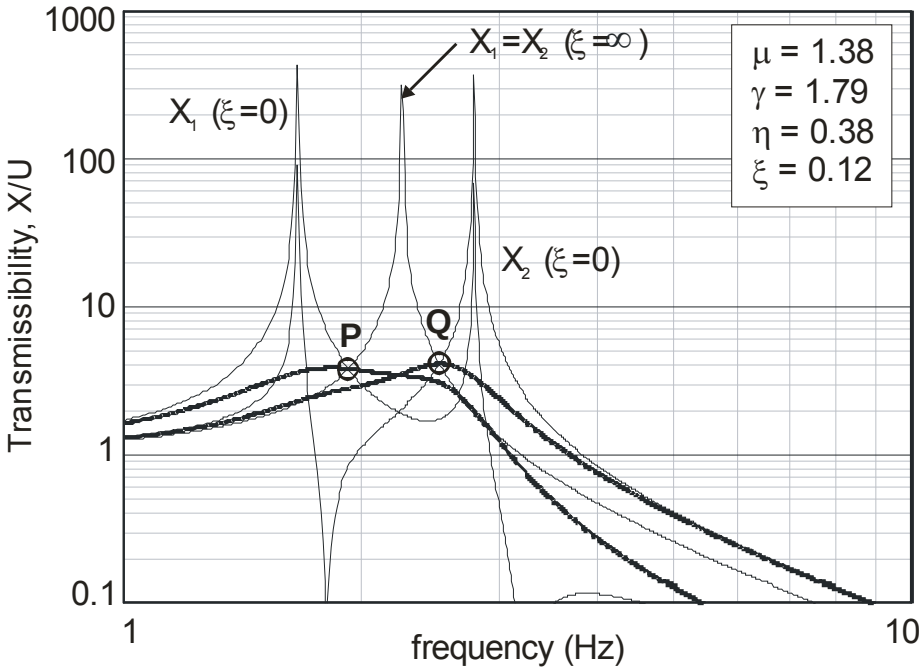

Figure 3.5 Optimized transmissibility for prototype structure defined by Trial #3-16.

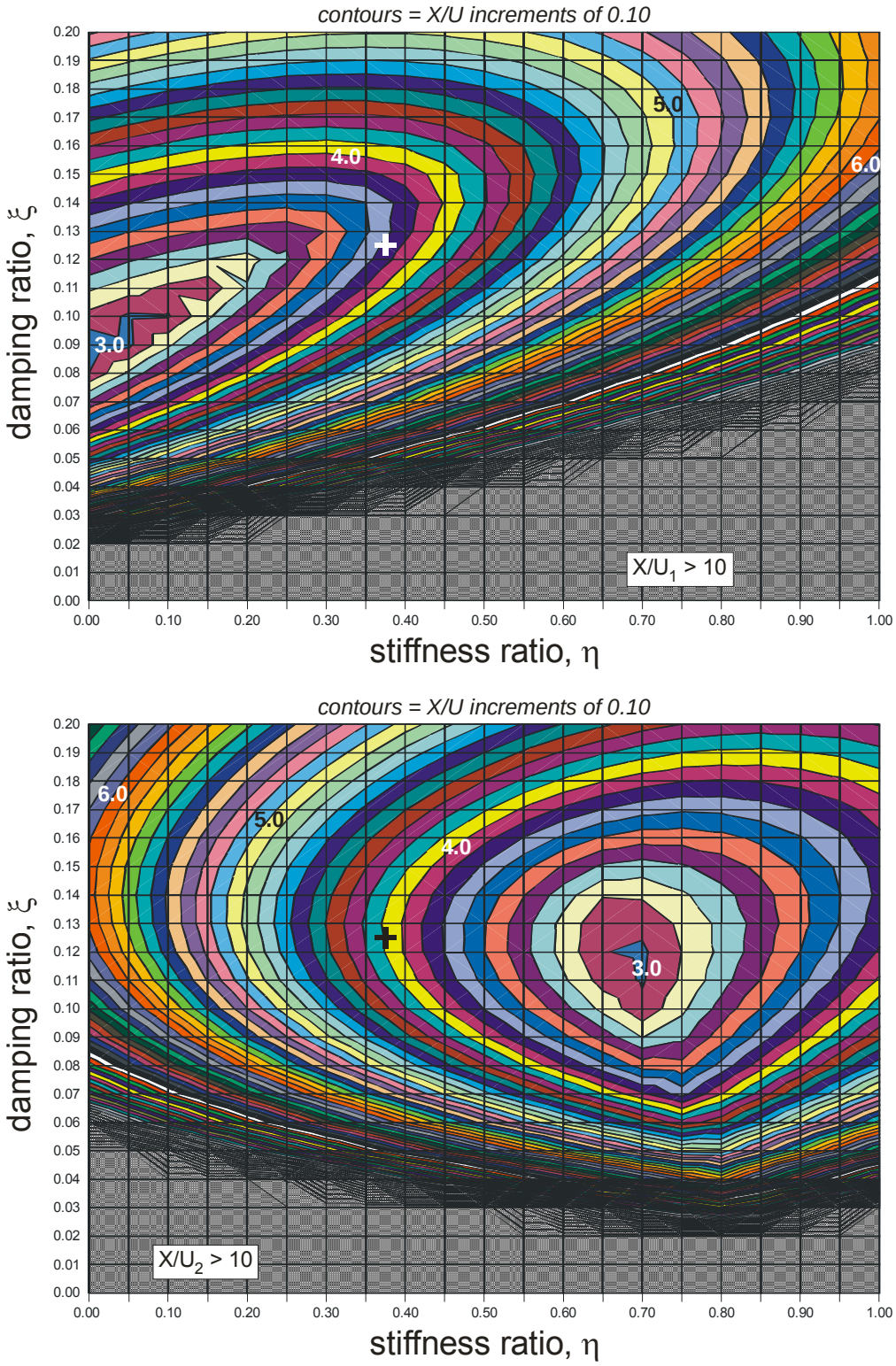

Figure 3.6 Transmissibility of individual wall piers E (top) and D (bottom) over range of stiffness and damping. (Calculated optimized value for CCW D-E shown as +.)

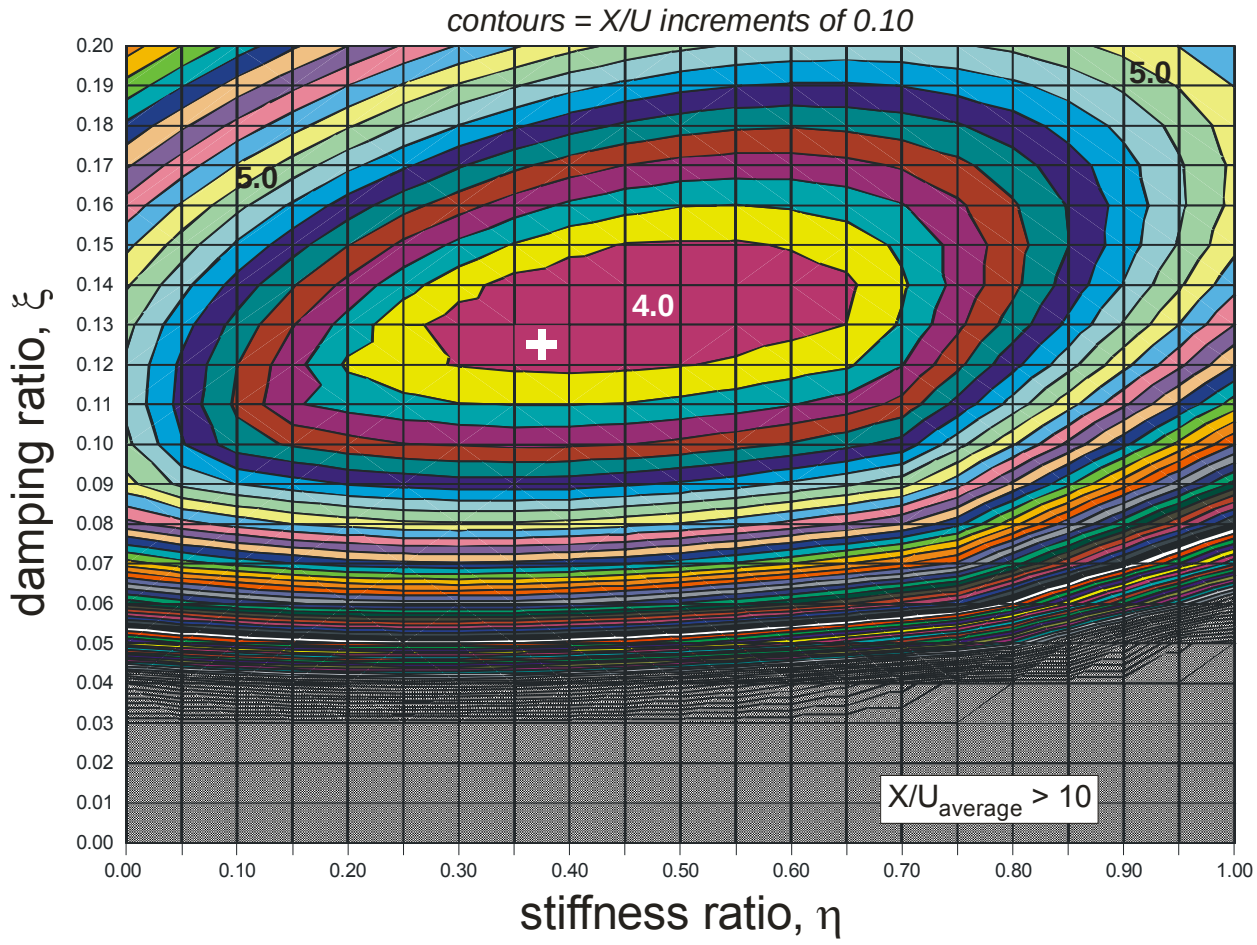

Figure 3.7 Average transmissibility of wall piers D and E over range of stiffness and damping. (Calculated optimized value for CCW D-E shown as +.)

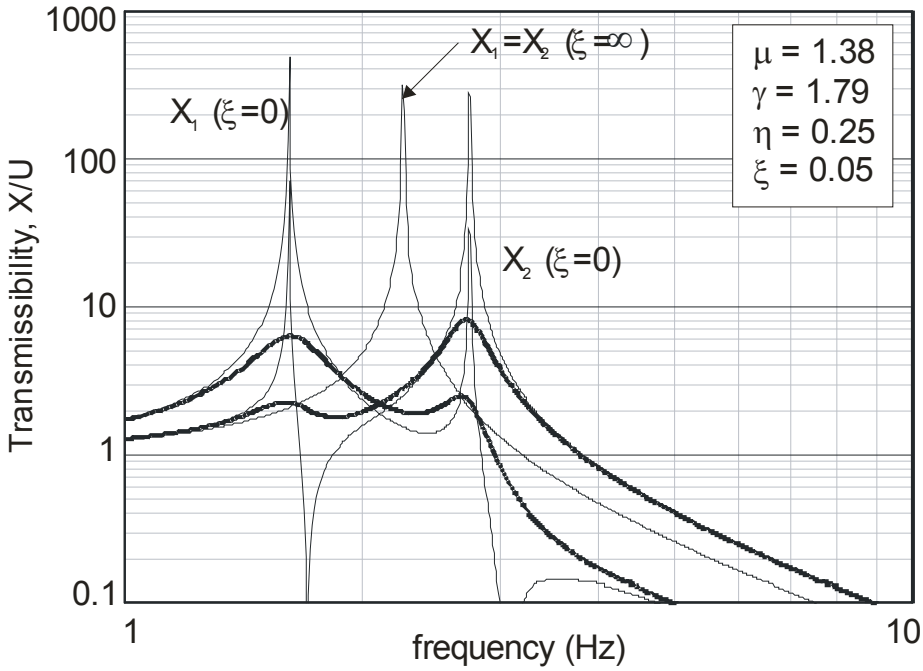

Figure 3.8 Transmissibility for prototype structure having $\xi = 0.050$ and $\eta = 0.250$.

4.0 LINEAR TIME HISTORY ANALYSES

To further examine the behavior of the optimized system, a 2DOF model representing Trial # 3-16 (described in Chapter 3) was subject to a linear time-history (LTH) analysis. Program RUAUMOKO (Carr, 2000) was used for this analysis. RUAUMOKO was selected largely for its ease of programming and extensive library of nonlinear hysteretic behaviors available for future analytical study associated with this preliminary research study. The 2DOF system was modeled as shown in Figure 4.1, and was assumed to remain elastic. The input ground motion used was that recorded from the 1940 El Centro earthquake (north-south direction) shown in Figure 4.2. For comparison, three additional coupling scenarios were modeled and subjected to the earthquake simulation: the arbitrary coupling described in Chapter 3.5.1 (Figure 4.1); a scenario with no coupling; and a scenario having rigid coupling. Finally, in order to investigate the effect of a greater natural frequency ratio, the same scenarios were carried out from the wall combination of Trial #3-4 (Wall E to Wall A, shown in Figure 4.5).

4.1 TWO-DOF SYSTEM MODELING

For both wall combinations, the individual wall piers were simplified to equivalent SDOF systems, as discussed in Chapter 3. The properties of these SDOF systems are tabulated in Appendix B and shown in Figures 4.1 and 4.5. For modeling, the coupled 2DOF system was set up using unit column heights and lateral separation. This was done for simplicity of modeling but does result in artificial deflection and internal force values arising from the modeling. It is important to note that the deflections reported throughout this chapter are based on a building having unit (1 m) height and *are not intended to be representative of a practical structure*. The intent of this chapter is to draw comparisons between coupled systems and thus relative values

between models are relevant. All models were developed with the same artificial unit parameters and may thus be compared directly with each other.

Beam elements were used to model the wall piers as sway columns. Since no vertical DOFs were considered, no axial load-moment interaction was considered (although RUAUMOKO is able to model this with ease). The wall piers were assumed to be concrete, and were assigned 5% "initial stiffness Rayleigh damping" (Carr, 2000). The required input values for the wall pier properties were as follows:

E = 28.5 GPa

$$I = \frac{kh^3}{12E} \tag{4.1}$$

where k is the equivalent SDOF wall pier stiffness determined by equation 3.7 (in this case reduced to account for cracking) and h = 1 m. The wall piers were assumed to be elastic elements for this study. The equivalent SDOF mass determined by equation 3.5 is lumped at the single lateral DOF at the top of each wall pier.

The tops of the columns were connected by a horizontal linear spring element having the spring stiffness calculated by equation 3.26, and a horizontal linear damping element (dashpot) having the damping value calculated by (see equation 2.19):

$$c_d = \xi \cdot 2 \cdot \sqrt{m2 \cdot k2} \tag{4.2}$$

For each wall pair (E-D and E-A), four coupling scenarios were considered:

1. Optimized: using values obtained from the fixed point analysis (Chapter 3).
2. Arbitrary: using values of $\xi = 0.050$ and $\eta = 0.250$.
3. No Coupling: the walls are modeled as individual SDOF having no coupling stiffness or damping.
4. Rigid Link: the walls are "pinned" together with a rigid link.

To achieve infinite damping and stiffness in the rigid coupling scenario, the 2DOFs (Figure 4.1) were constrained together, forcing the DOFs to displace the same distance. Table 4.1 summarizes the damping and stiffness values used for all four scenarios for each wall combination.

Each system was subject to the north-south direction ground motion record from the 1940 El Centro earthquake (record obtained by Carr 2000). The twenty-second ground motion record is digitized at 0.01 seconds. The time-step used in the elastic analysis was 0.002 seconds

although output is only recorded every 5 time steps, resulting in output also being digitized at 0.01 seconds.

4.2 WALL E - WALL D LINEAR TIME HISTORY RESULTS

The modeling was carried out for the wall combination from Trial 3-16, and the resulting DOF displacement time histories are shown in Figure 4.3 for each coupling scenario. The maximum displacement for each scenario is tabulated in Table 4.2.

Fixed point theory, described in Chapter 2, examines the effect of coupling a stiff structure to a more flexible structure. A coupling stiffness and damping that optimizes the response of the system as a whole is determined. The interaction between SDOF systems allowed by the coupling stiffness and damping results in the flexible structure becoming apparently stiffer at the expense of the stiffer structure. Thus the coupled system has an overall (or global) stiffness which lies between the individual wall pier stiffnesses and the sum of these stiffnesses.

The expected response of the 2DOF system, therefore, is that the optimal coupling stiffness and damping will result in the optimal gain or loss of stiffness in the flexible or stiffer structures, respectively, resulting in improved global behavior. Thus it should be expected that the optimized structure exhibits improved global behavior over all other scenarios. Nonetheless, as clearly shown in Figure 4.6, the behavior of either individual pier is not optimized under the optimized condition: in particular the stiffer wall deflection may in fact increase as it interacts with the more flexible wall. In order to illustrate this effect, the overall or global behavior of each system will be represented by the simple average of the individual wall pier displacements. Additionally, in this discussion it is important to note that due the nature of the solution used (i.e: the requirement that $\omega_2/\omega_1 > 1.0$), Wall E, in both reported cases, is the more flexible pier.

Figure 4.3 shows the wall pier responses of each scenario considered. Qualitative investigation of the displacement time histories indicates that increased coupling (in this case, progressing from none, to Arbitrary, to Optimal, to Rigid) results in the wall behaviors becoming increasingly in phase. The No Coupling plot in Figure 4.3 clearly shows each wall behaving individually and the resulting out-of-phase behavior expected as a result of the frequency ratio, γ.

Table 4.2 summarizes the peak displacements observed for each scenario in addition to the average displacement in each case. The behavior described above is clearly illustrated in Table 4.2 where Wall E is the more flexible wall. Using the No Coupling scenario as a baseline, the optimized displacement of Wall E has fallen (improved) 32.5% at the expense of an increase in Wall D displacement of only 0.4%. The average displacement has improved 24.7%. This latter value is the theoretical optimal improvement which may be affected by coupling these wall piers. In the Arbitrary scenario considered, both walls exhibit improved performance: 15.7% and 19.5% for Walls E and D, respectively, although the global improvement is only 16.7% - less than the optimal value.

It is instructive to also consider the Rigid Link scenario. In this scenario, the global stiffness is maximized as the sum of the individual wall pier stiffnesses. This maximization, however, does not result in an optimal behavior (global improvement of only 17.5%). More significantly, this scenario may result in a significant increase in the displacement of the stiffer wall as the loads are now shared in proportion to the wall stiffness. In the scenario shown in Table 4.2, Wall D displacement increases (reduced performance) 71.8%.

As alluded to earlier in this work, choosing values of coupling stiffness and damping that are less than optimal will result in overall system response that is less than optimal. Additionally, the selection of optimal values may simply be unrealistic. For example, obtaining an optimal damping value of $\xi = 0.125$ is not possible for a typical structure without mechanical damping devices being used. A realistic value of damping for a well-detailed concrete wall structure is likely about $\xi = 0.050$ (Newmark and Hall, 1982) as is used in the Arbitrary scenario. The results shown in Figure 4.3 and Table 4.2 suggest that although an optimal performance may be achieved, there is a considerable range of parameters where “near optimal” performance may be achieved. In the case of walls D-E, it may be argued that there is not a significant difference in structural performance between the Optimal, Arbitrary, and Rigid Link scenarios, and all represent an improvement on the No Coupling scenario.

In comparing the behavior of the Optimized and Arbitrary scenarios, there is a clear benefit to Wall E when the system is optimized over the arbitrary and uncoupled scenarios. It is shown that Wall D behavior is marginally worse in the optimal scenario Figure 4.4 shows this relationship between the optimal and arbitrary scenarios for Wall D and Wall E. This result is expected, since the coupling should benefit the overall system by improving the more flexible

response, at the expense of the stiffer wall. The arbitrary scenario represents a more "structurally realistic" alternative than the optimal case; its average response is an improvement over the uncoupled response, although there is still a large spike in Wall E displacement at approximately 2.2 seconds into the earthquake. The specific dynamic behavior, in this case, is also a function of the input ground motion used. The El Centro record is known to have relatively uniform high spectral intensity at frequencies greater than 0.5 Hz – thus affecting the prototype structures considered relatively severely

4.3 WALL E - WALL A LINEAR TIME HISTORY RESULTS

The natural frequency ratio of $\gamma = 1.79$ for the Wall E to Wall D case (above) shows that the walls are not greatly dissimilar. In an attempt to show a greater disparity of wall performance across the scenarios, a second trial was chosen that would have very different responses to dynamic loading. Trial # 3-4 consists of Wall E coupled to Wall A (see Appendix B). The natural frequency ratio of this case, $\gamma = 2.54$, shows a more significant difference in the expected dynamic response of the individual wall piers. The four scenarios described above were run for this wall combination. The 2DOF model is shown in Figure 4.5. The coupling stiffness and damping values are tabulated in Table 4.1. As shown in Figure 4.6 and Table 4.3, the effect of increasing the frequency ratio of the structures resulted in a significant improvement in response for the flexible wall (Wall E) when the system was coupled. In this case, the stiffer wall (Wall A) behavior is also improved for the Optimized and Arbitrary scenarios. As expected (see above) the stiff wall behavior is worse for the Rigid Link scenario where the forces are now carried in a manner proportional to wall stiffness. Figure 4.7 shows the dramatic improvement in Wall E behavior and the relatively minor effect on Wall A behavior for the Optimal and Arbitrary scenarios. In the Optimal scenario, Wall E experiences a 77.4% decrease in displacement over the No Coupling scenario while Wall A experiences a 15.2% decrease in displacement. The average displacement improvement is 69.3% for the optimal case.

Despite the significant change in stiffness (a reduction of 85%) from the Optimal to Arbitrary scenarios, the overall performance improvement remained significant. From Table 4.3, the Wall E response was improved by 53.7%, while the Wall A response improved by 17.9%.

This follows the results of the Wall E-Wall D case, as the stronger wall response improved more with this change in coupling. But, as in the previous combination, the average arbitrary response is less than that of the optimal; a 49% reduction vs. the optimal 69.3% reduction. This result, again illustrates the reasonable large range of parameters across which improved or near-optimal behavior may be achieved.

Table 4.1 Parameters used to model stiffness and damping links (see Figures 4.1 and 4.5).

Coupling Scenario		Wall Combination							
		Wall E - Wall D				Wall E - Wall A			
		η	k (N/m)	ξ	c_d (Ns/m)	η	k (N/m)	ξ	c_d (Ns/m)
1	Optimized	0.378	9.90×10^8	0.125	1.73×10^8	1.674	4.38×10^9	0.112	2.88×10^8
2	Arbitrary	0.250	6.50×10^8	0.050	6.90×10^7	0.250	6.55×10^8	0.050	1.30×10^8
3	No Coupling	0	0	0	0	0	0	0	0
4	Rigid Link	∞	∞	∞	∞	∞	∞	∞	∞

Table 4.2 Wall E to Wall D summary of peak lateral displacements for coupling scenarios.

	Coupling Scenario for $\gamma = 1.79$			
	Optimal	Arbitrary	No Coupling	Rigid Link
Wall E Displacement (cm)	5.14	6.42	7.62	4.14
Wall D Displacement (cm)	2.42	1.94	2.41	4.14
Average Displacement (cm)	3.78	4.18	5.02	4.14

Table 4.3 Wall E to Wall A summary of peak lateral displacements for coupling scenarios.

	Coupling Scenario for $\gamma = 2.54$			
	Optimal	Arbitrary	No Coupling	Rigid Link
Wall E Displacement (cm)	1.72	3.52	7.60	1.48
Wall A Displacement (cm)	0.95	0.92	1.12	1.48
Average Displacement (cm)	1.34	2.22	4.36	1.48

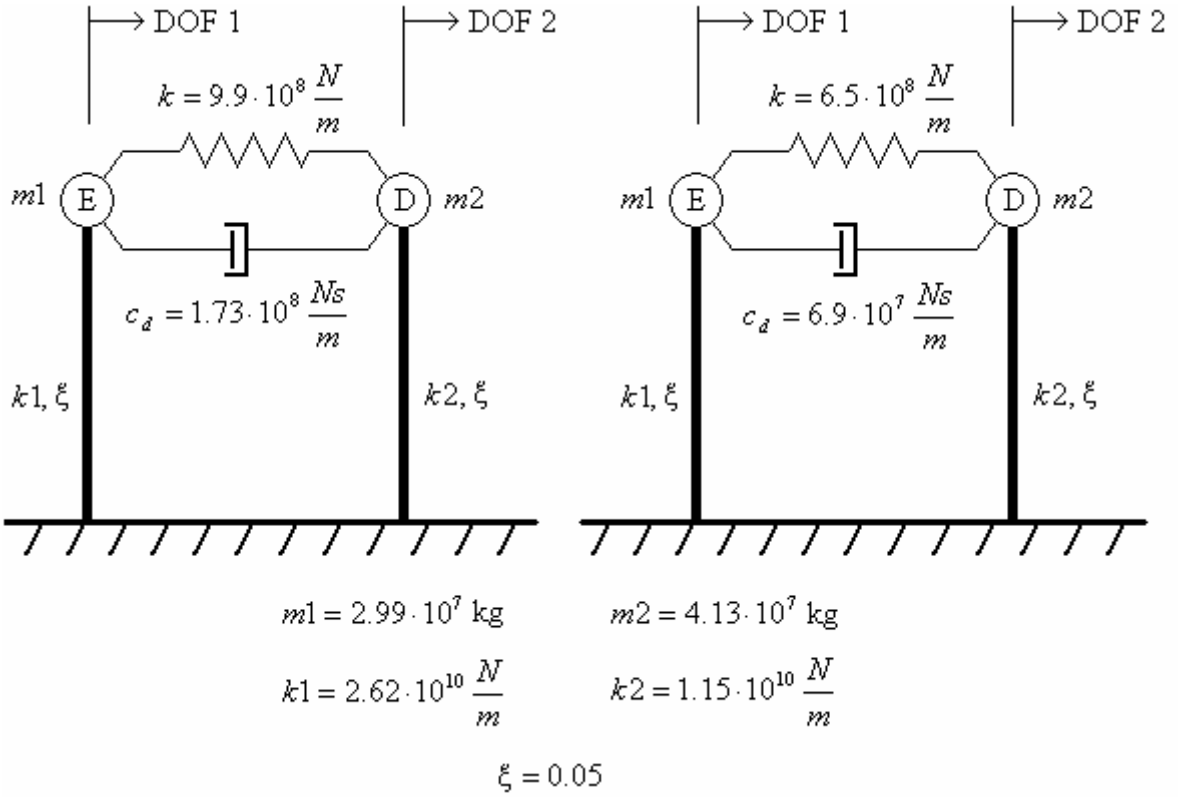

Figure 4.1 Schematic of Optimized (left) and Arbitrary (right) prototype structures for wall combination from Trial # 3-16.

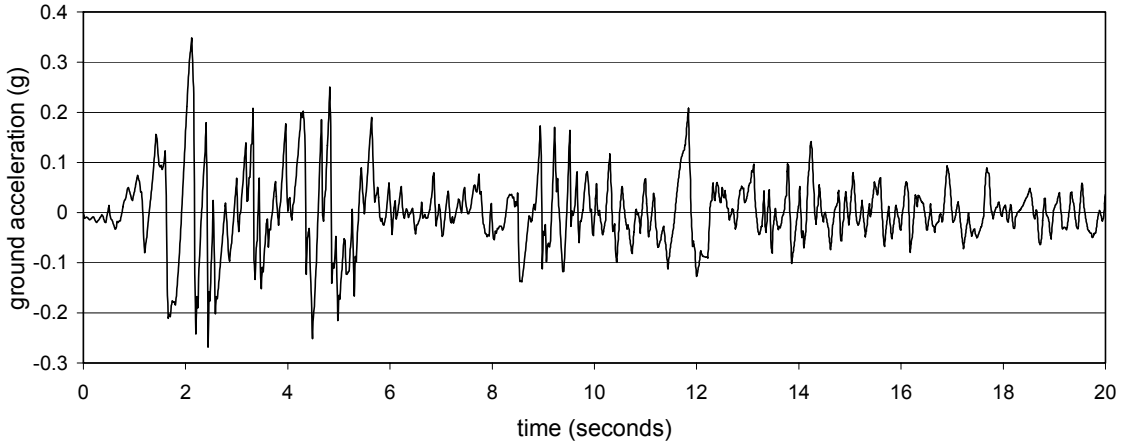

Figure 4.2 1940 El Centro (NS) ground motion record (obtained from Carr, 2000).

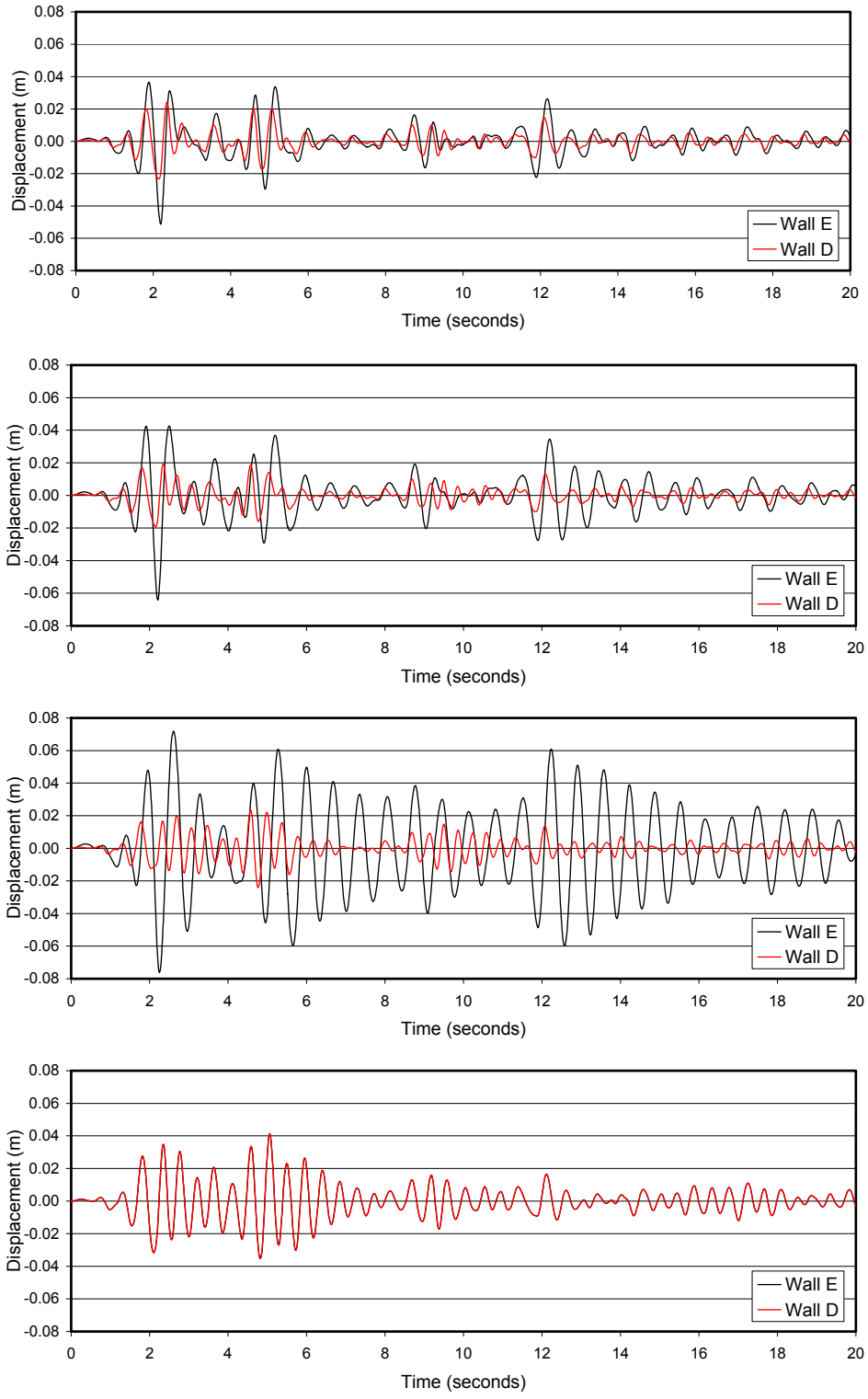

Figure 4.3 Lateral displacement response of Trial # 3-16.
Scenarios from the top down: Optimized, Arbitrary, No Coupling, Rigid Link.

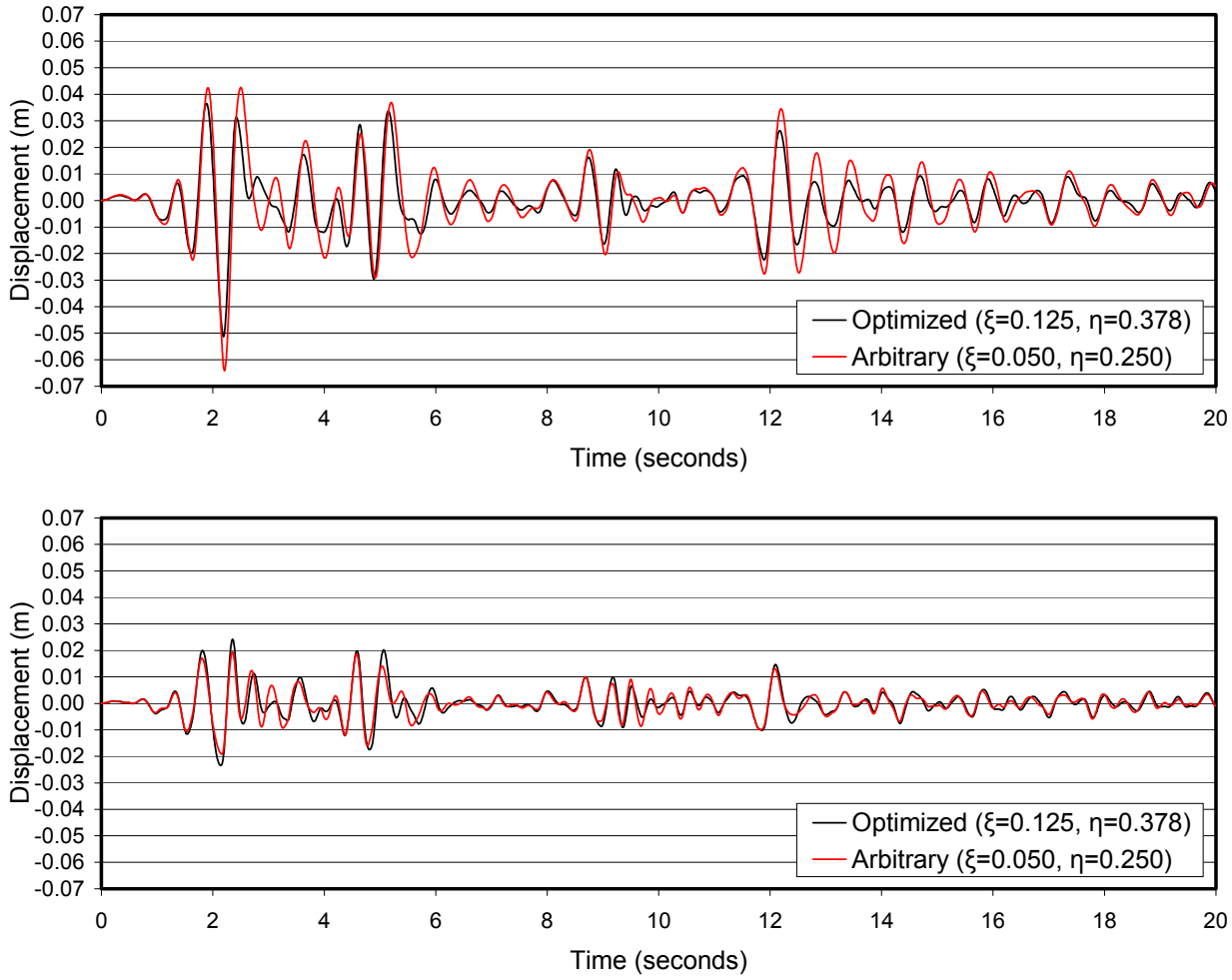

Figure 4.4 Response of Optimized vs. Arbitrary scenarios for Trial 3-16.
Wall E on top, Wall D on bottom.

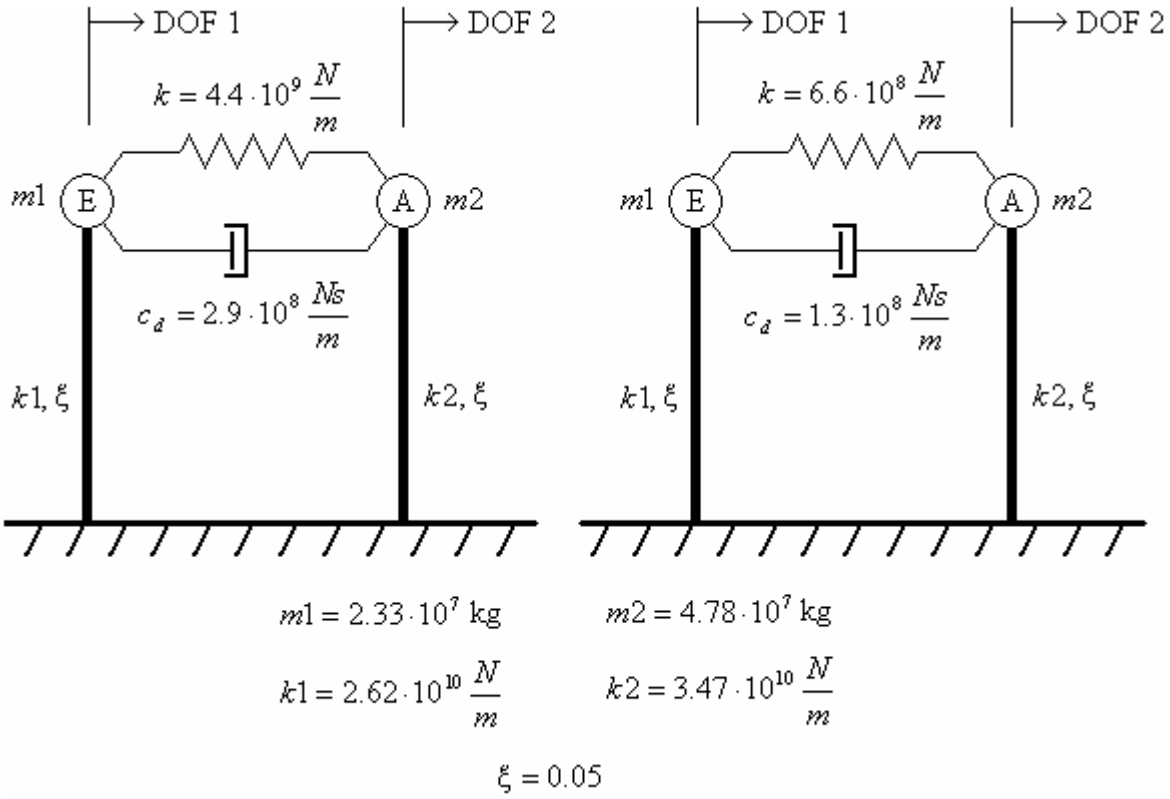

Figure 4.5 Schematic of Optimized (left) and Arbitrary (right) prototype structures for wall combination from Trial # 3-4.

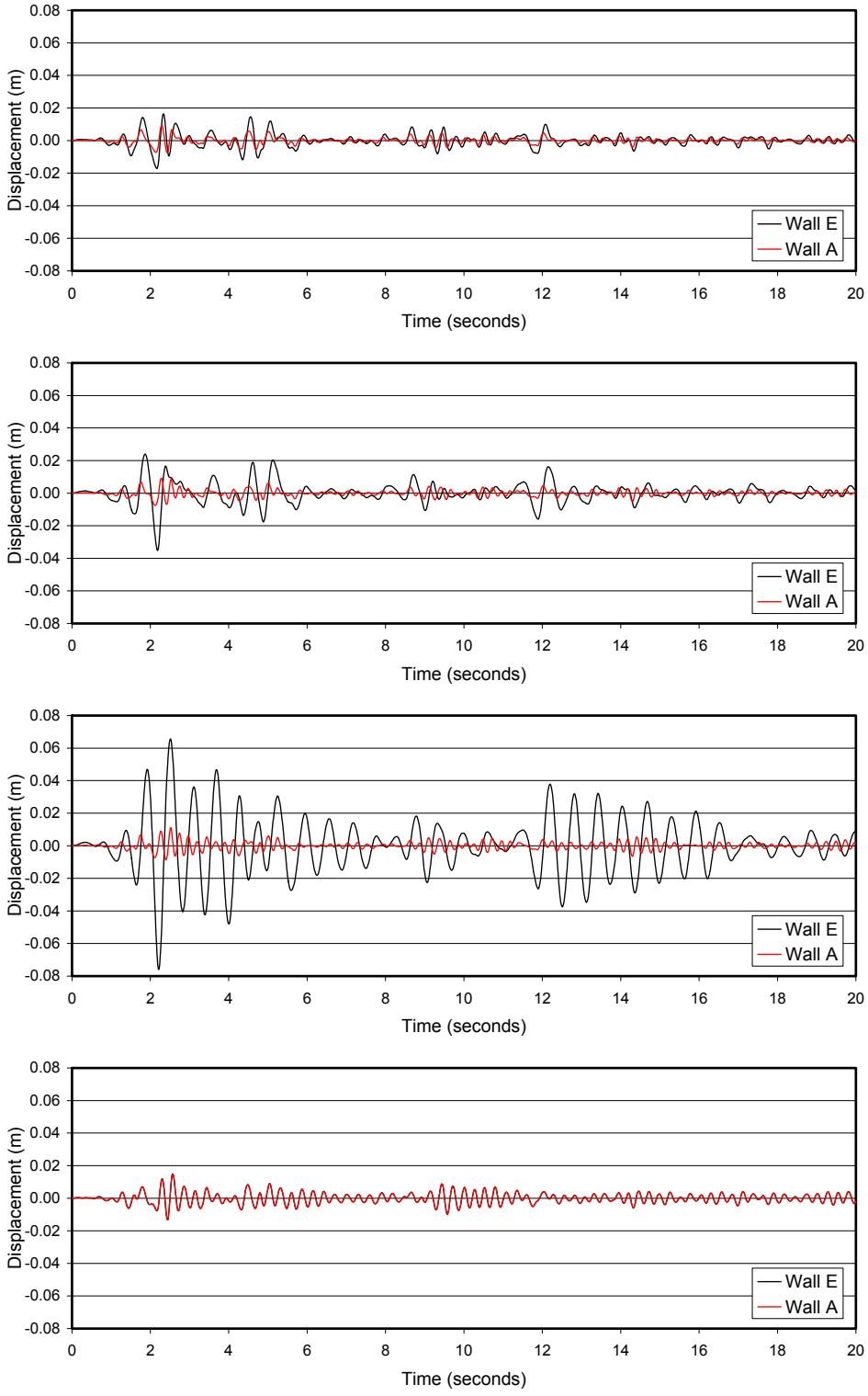

Figure 4.6 Lateral displacement response of Trial # 3-4.
Scenarios from the top down: Optimized, Arbitrary, No Coupling, Rigid Link.

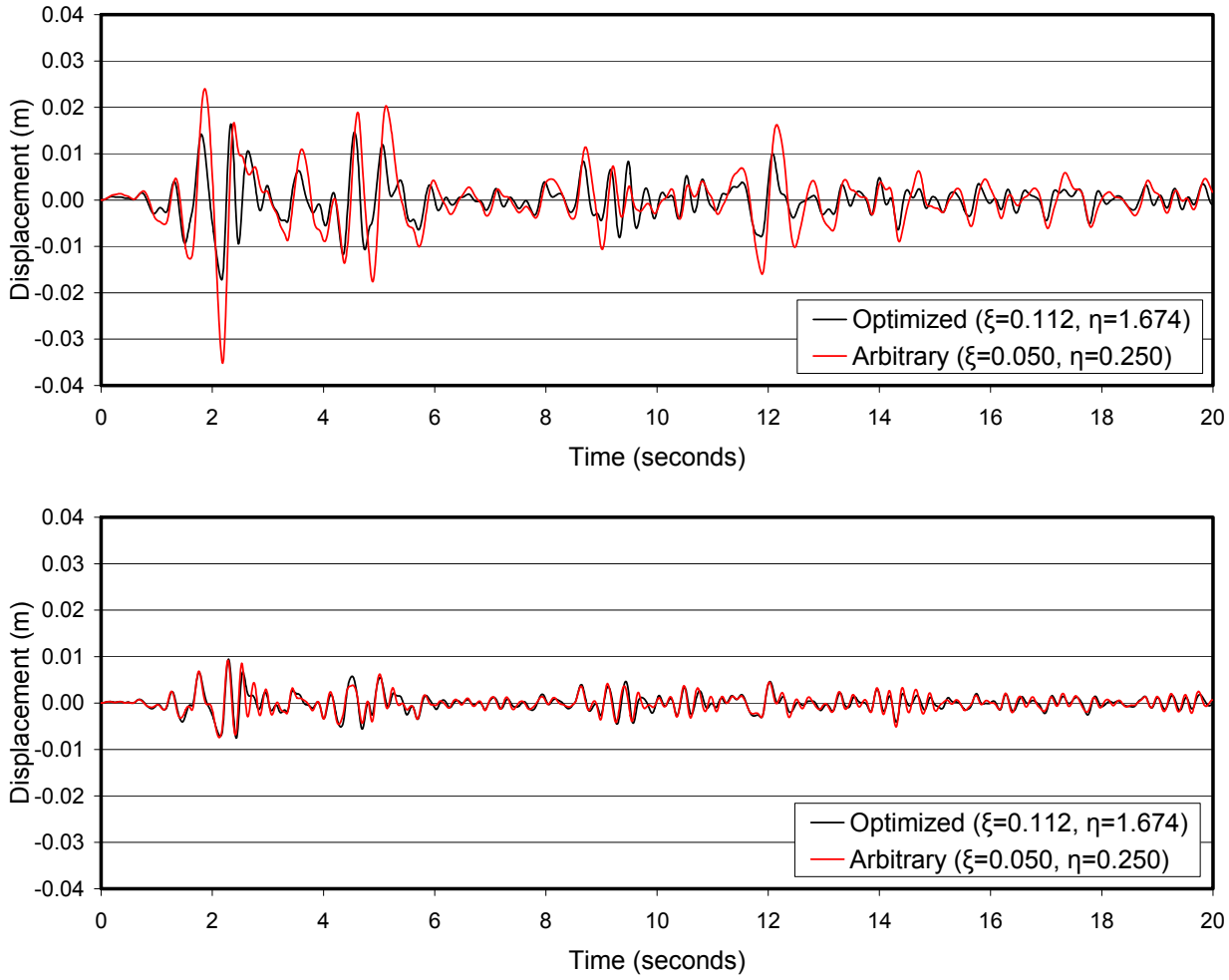

Figure 4.7 Response of Optimized vs. Arbitrary scenarios for Trial 3-4.
Wall E on top, Wall A on bottom.

5.0 CONCLUSIONS AND FUTURE RESEARCH DIRECTIONS

The objective of this work is to present a preliminary exploration of the use of Fixed Point Theory as a means of optimizing coupled core wall (CCW) behavior. The performance objective attained through optimization is the minimization of transmissibility of ground motion displacement. The principles discussed in Chapter 2 can be used to apply fixed point theory to coupled core walls, as shown in Chapters 3 and 4. By converting two MDOF wall pier structures into equivalent SDOF systems and applying the closed form solution for fixed point theory, optimal coupling stiffness and damping are determined for the resulting CCW. Specific wall combinations presented in Chapter 4 show a noted improvement in the Optimized and Arbitrary scenarios over the No Coupling scenario. Fixed point theory was clearly useful in finding the best improvement in the overall system response of the coupled walls. The optimal system behavior does not coincide with the optimal behavior of the individual wall piers. Although not discussed here, it should be clear from Chapter 3 and specifically Figure 3.6 that the same method may be employed to optimize a single wall pier behavior without regard for the optimal behavior of the other pier or system as a whole. Such an approach of component and/or system optimization is compatible with a performance-based design approach. Future research in this area will illuminate this approach further.

Specific conclusions of this study are as follows:

1. The approach used is only applicable to systems with component wall piers having different dynamic properties. When the natural frequency ratio, γ, approaches 1.0, ω_1 approaches equality with ω_2. This condition causes equation 3.11 to approach zero, resulting in the calculated fixed point stiffness ratio (equation 3.10) to also approach zero. This represents the trivial case where two identical SDOF systems will have continued identical dynamic behavior (and thus equal transmissibility) regardless of the level of coupling and/or damping provided.

2. Related to the previous conclusion, when the product of mass and frequency ratios, $\mu\gamma$, falls below 1.0, the optimization process yields negative stiffness values. Although mathematically correct, such results are not physically meaningful – indicating a negative stiffness is required for optimization. In essence, coupling the wall piers in this case results in increased transmissibility compared to the uncoupled walls.
3. The parametric study results (Chapter 3) show that there is little difference between the four cases considered. This is a reflection of the fact that the formulation of fixed point theory relies mostly on ratios of dynamic properties between two equivalent SDOF systems. This observation may permit eventual generalization of the approach in a manner analogous to spectral analysis methods.
4. Regardless of ratios of properties, numeric values of optimized stiffness and damping are reduced when cracked concrete section properties are used. This should be expected since the cracked structure is more flexible and thus requires less coupling to affect the same improvement in behavior.
5. As the frequency ratio, γ, increases; that is: the wall pier dynamic properties are less similar, the optimized stiffness and damping values required for optimization increase. This observation may effectively impose an upper limit on the frequency ratio for practical structural systems since both damping and stiffness will have practical limits based on structural geometry.
6. Regardless of the previous conclusions, although optimization may not be practical outside of a range of parameters, improved transmissibility is still quite viable – the solution is simply not optimized. Furthermore, it is shown that the range of reasonable transmissibility values or "near-optimal" behavior may encompass a relatively wide range of parameters.
7. Fixed point theory examines the effect of coupling a stiff structure to a more flexible structure. A coupling stiffness and damping that optimizes the response of the system as a whole is determined. The interaction between SDOF systems allowed by the coupling stiffness and damping results in the flexible structure becoming apparently stiffer at the expense of the stiffer structure. Thus the coupled system has an overall (or global) stiffness which lies between the individual wall pier stiffnesses and the sum of these stiffnesses.

8. Although individual wall pier behavior is not optimized at the calculated optimal coupling stiffness and damping, the average behavior of the walls is. This optimal improvement in performance may also be used in a performance based designed scenario to assess the relative benefits of coupling wall structures.

5.1 FUTURE RESEARCH DIRECTIONS

This study was a pilot study initiated to develop an understanding of the optimization of dynamic properties of coupled wall structures. A fundamental assumption of all structural analysis of coupled walls is that the axial behavior of the coupling elements is essentially rigid. This is the rigid diaphragm assumption used in high-rise building analysis. Clearly, in reality, no diaphragm is rigid. In this study, a method for investigating the effects of a non-rigid coupling element is explored and shown to have a potentially significant effect on the dynamic performance of the structure and its component piers. To adequately place these results in context, it is necessary to understand the "real" stiffness and damping provided by coupling beams in CCW systems and even by slabs in uncoupled systems of wall piers.

The results of this study have suggested a number of applications within a performance-based design concept where optimization of dynamic properties (or at least the understanding of what is necessary to optimize properties) could be used in design. Most significantly, the concept proposed by Harries et al. (2004b) where a CCW may have fundamentally different structural behavior at different hazard levels (see Section 2.1.3) may be supported by the present work. Expected changes in dynamic performance may be predicted in a manner similar to that explored in Chapter 4, for instance.

To properly extend this study the following steps should be taken:

1. Expand the modeling from a pair of equivalent SDOF piers to a pair of MDOF wall piers. The distribution of coupling stiffness and damping must be investigated in this case to determine, the optimal vertical distribution. As a point of initiation, a distribution reflecting the first mode deflected shape may be appropriate. Continued studies may consider a "modal" approach to stiffness and damping distribution.

2. Extend the study to investigate nonlinear effects.
3. Consider a wider variation of structural parameters such as building height. Considering piers of different height in the same structure may also be considered.

Finally, this study is essentially concerned with using interaction forces and damping to control the dynamic properties of a multi-structure system. The problem itself may be better applied to other structures besides CCWs. Bridge piers and slender structures may offer appropriate applications.

APPENDIX A

EXAMPLE CALCULATION OF SDOF SYSTEM AND OPTIMIZATION PROCESS

Comparison of Wall D to Wall E at 12 Stories With Cracked Walls

Moments of Inertia:

From Table 3.1, designate Wall D to be wall 1 and designate Wall E as wall 2.

$I1 := 26.5653\ m^4$

$I2 := 6.0291\ m^4$

Case Numbers:

* Cases defined in Table 3.2.

Case 1: 12 Floors, no change to EI.
Case 2: 24 Floors, no change to EI.
Case 3: 12 Floors, modified EI for first 2 floors.
Case 4: 24 Floors, modified EI for first 3 floors.

To simulate the 12 story structure with cracked walls, use Case 3.

$Case := 3$

Number of Floors:

The number of floors is automatically assigned based on the case number.

$floors := if(Case = 1 \vee Case = 3, 12, 24)$

$floors = 12$

Areas:

From Table 3.1, designate Wall D to be wall 1 and designate Wall E as wall 2.

$A1 := 11.005\ m^2$

$A2 := 7.965\ m^2$

28.5 GPa must be converted to N/m^2:

$E := 28.5 \cdot 10^9\ N/m^2$

Story height:

$h := 3.60\ m$

Assumed story weight:

$WTtot := 10000\,Mg$ $\quad WTtot = 1 \times 10^4$ Mg Total weight of floor

The total weight of the floor must be divided up between the two walls according to the cross sectional area distribution. The weight is then converted into kilo-grams from mega-grams.

$$m1 := \frac{A1}{A1 + A2} \cdot WTtot \cdot 1000 \qquad m1 = 5.801 \times 10^6 \text{ kg}$$

$$m2 := \frac{A2}{A1 + A2} \cdot WTtot \cdot 1000 \qquad m2 = 4.199 \times 10^6 \text{ kg}$$

The stiffness of each wall must also be calculated:

The wall stiffness is calculated. See Section 2.1.

$$k1 := \left(\frac{12 \cdot E \cdot I1}{h^3} \right) \qquad k1 = 1.947 \times 10^{11} \text{ N/m}$$

$$k2 := \left(\frac{12 \cdot E \cdot I2}{h^3} \right) \qquad k2 = 4.419 \times 10^{10} \text{ N/m}$$

First Mode Response Calculation for Wall 1 and Wall 2

-This portion of the worksheet calculates equivalent SDOF mass of the MDOF system based on the eigenvector method described in Seto et al. (1987).

-The worksheet only handles shear buildings of any height having uniform mass and two regions of different stiffness.

-More complex structures require the M and K matrices to be assembled manually or by using an advanced algorithm.

Assemble M and K matrices for both walls: * Note: Mass matricies are diagonal.

$$M1 := \left| \begin{array}{l} \text{for } i \in 1 .. floors \\ \quad M1_{i,i} \leftarrow m1 \\ M1 \end{array} \right. \qquad M2 := \left| \begin{array}{l} \text{for } i \in 1 .. floors \\ \quad M2_{i,i} \leftarrow m2 \\ M2 \end{array} \right.$$

Alter the stiffness based on the case number (modified EI for cases 3 and 4):

Stiffness coefficient for cracked floors (Both adjustment factors are independent of the wall number):

$$\alpha l := \text{if}(\text{Case} = 3 \vee \text{Case} = 4, 0.35, 1)$$

Stiffness coefficient for remaining (upper) floors:

$$\alpha u := \text{if}(\text{Case} = 3 \vee \text{Case} = 4, 0.70, 1)$$

Floor level at which hinge behavior diminishes:

$$\text{rfloors} := \text{if}(\text{Case} = 1 \vee \text{Case} = 3, 2, 3)$$

$K1 :=$

for $i \in 2 .. (\text{rfloors})$

- $K1_{i,i} \leftarrow 2k1 \cdot \alpha l$
- $K1_{i,i+1} \leftarrow -k1 \cdot \alpha l$
- $K1_{i,i-1} \leftarrow -k1 \cdot \alpha l$

for $i \in (\text{rfloors} + 1) .. (\text{floors} - 1)$

- $K1_{i,i} \leftarrow 2k1 \cdot \alpha u$
- $K1_{i,i+1} \leftarrow -k1 \cdot \alpha u$
- $K1_{i,i-1} \leftarrow -k1 \cdot \alpha u$

$K1_{\text{rfloors},\text{rfloors}-1} \leftarrow -k1 \cdot \alpha l$

$K1_{\text{rfloors},\text{rfloors}+1} \leftarrow -k1 \cdot \alpha u$

$K1_{\text{rfloors},\text{rfloors}} \leftarrow k1 \cdot (\alpha l + \alpha u)$

$K1_{1,1} \leftarrow 2k1 \cdot \alpha l$

$K1_{1,2} \leftarrow -k1 \cdot \alpha l$

$K1_{\text{floors},\text{floors}} \leftarrow k1 \cdot \alpha u$

$K1_{\text{floors},(\text{floors}-1)} \leftarrow -k1 \cdot \alpha u$

$K1$

$K2 :=$

for $i \in 2 .. (\text{rfloors})$

- $K2_{i,i} \leftarrow 2k2 \cdot \alpha l$
- $K2_{i,i+1} \leftarrow -k2 \cdot \alpha l$
- $K2_{i,i-1} \leftarrow -k2 \cdot \alpha l$

for $i \in (\text{rfloors} + 1) .. (\text{floors} - 1)$

- $K2_{i,i} \leftarrow 2k2 \cdot \alpha u$
- $K2_{i,i+1} \leftarrow -k2 \cdot \alpha u$
- $K2_{i,i-1} \leftarrow -k2 \cdot \alpha u$

$K2_{\text{rfloors},\text{rfloors}-1} \leftarrow -k2 \cdot \alpha l$

$K2_{\text{rfloors},\text{rfloors}+1} \leftarrow -k2 \cdot \alpha u$

$K2_{\text{rfloors},\text{rfloors}} \leftarrow k2 \cdot (\alpha l + \alpha u)$

$K2_{1,1} \leftarrow 2k2 \cdot \alpha l$

$K2_{1,2} \leftarrow -k2 \cdot \alpha l$

$K2_{\text{floors},\text{floors}} \leftarrow k2 \cdot \alpha u$

$K2_{\text{floors},(\text{floors}-1)} \leftarrow -k2 \cdot \alpha u$

$K2$

The first 6 columns for each stiffness matrix is shown below:

K1 =

	1	2	3	4	5	6
1	$1.363 \cdot 10^{11}$	$-6.816 \cdot 10^{10}$	0	0	0	0
2	$-6.816 \cdot 10^{10}$	$2.045 \cdot 10^{11}$	$-1.363 \cdot 10^{11}$	0	0	0
3	0	$-1.363 \cdot 10^{11}$	$2.726 \cdot 10^{11}$	$-1.363 \cdot 10^{11}$	0	0
4	0	0	$-1.363 \cdot 10^{11}$	$2.726 \cdot 10^{11}$	$-1.363 \cdot 10^{11}$	0
5	0	0	0	$-1.363 \cdot 10^{11}$	$2.726 \cdot 10^{11}$	$-1.363 \cdot 10^{11}$
6	0	0	0	0	$-1.363 \cdot 10^{11}$	$2.726 \cdot 10^{11}$
7	0	0	0	0	0	$-1.363 \cdot 10^{11}$
8	0	0	0	0	0	0
9	0	0	0	0	0	0
10	0	0	0	0	0	0
11	0	0	0	0	0	0
12	0	0	0	0	0	0

K2 =

	1	2	3	4	5	6
1	$3.094 \cdot 10^{10}$	$-1.547 \cdot 10^{10}$	0	0	0	0
2	$-1.547 \cdot 10^{10}$	$4.64 \cdot 10^{10}$	$-3.094 \cdot 10^{10}$	0	0	0
3	0	$-3.094 \cdot 10^{10}$	$6.187 \cdot 10^{10}$	$-3.094 \cdot 10^{10}$	0	0
4	0	0	$-3.094 \cdot 10^{10}$	$6.187 \cdot 10^{10}$	$-3.094 \cdot 10^{10}$	0
5	0	0	0	$-3.094 \cdot 10^{10}$	$6.187 \cdot 10^{10}$	$-3.094 \cdot 10^{10}$
6	0	0	0	0	$-3.094 \cdot 10^{10}$	$6.187 \cdot 10^{10}$
7	0	0	0	0	0	$-3.094 \cdot 10^{10}$
8	0	0	0	0	0	0
9	0	0	0	0	0	0
10	0	0	0	0	0	0
11	0	0	0	0	0	0
12	0	0	0	0	0	0

Calculate Eigenvalues:

$$\Lambda 1 := \mathrm{sort}\left(\mathrm{eigenvals}\left(M1^{-1} \cdot K1\right)\right) \qquad \Lambda 2 := \mathrm{sort}\left(\mathrm{eigenvals}\left(M2^{-1} \cdot K2\right)\right)$$

$\Lambda 1 =$

	1
1	279.75
2	$2.714 \cdot 10^3$
3	$7.954 \cdot 10^3$
4	$1.548 \cdot 10^4$
5	$2.35 \cdot 10^4$
6	$3.193 \cdot 10^4$
7	$4.298 \cdot 10^4$
8	$5.541 \cdot 10^4$
9	$6.76 \cdot 10^4$
10	$7.838 \cdot 10^4$
11	$8.68 \cdot 10^4$
12	$9.215 \cdot 10^4$

$\Lambda 2 =$

	1
1	87.723
2	851.18
3	$2.494 \cdot 10^3$
4	$4.855 \cdot 10^3$
5	$7.368 \cdot 10^3$
6	$1.001 \cdot 10^4$
7	$1.348 \cdot 10^4$
8	$1.737 \cdot 10^4$
9	$2.12 \cdot 10^4$
10	$2.458 \cdot 10^4$
11	$2.722 \cdot 10^4$
12	$2.89 \cdot 10^4$

Calculate Eigenvectors (mode shapes):

$\Phi 1 :=$ for $j \in 1 .. \mathrm{floors}$
$\quad \Phi 1^{\langle j \rangle} \leftarrow \mathrm{eigenvec}\left(M1^{-1} \cdot K1, \Lambda 1_j\right)$
$\Phi 1$

$\Phi 2 :=$ for $j \in 1 .. \mathrm{floors}$
$\quad \Phi 2^{\langle j \rangle} \leftarrow \mathrm{eigenvec}\left(M2^{-1} \cdot K2, \Lambda 2_j\right)$
$\Phi 2$

Set j to show the eigenvector for the first mode:

$$j := 1 .. 12$$

$\Phi 1_{j,1} =$

-0.078
-0.155
-0.191
-0.225
-0.257
-0.285
-0.31
-0.331
-0.348
-0.362
-0.371
-0.375

$\Phi 2_{j,1} =$

0.078
0.155
0.191
0.225
0.257
0.285
0.31
0.331
0.348
0.362
0.371
0.375

Normalize first mode by roof displacement:

$$\phi 1 := \left| \begin{array}{l} \text{for } j \in 1 .. \text{floors} \\ \quad \phi 1_{j,1} \leftarrow \dfrac{\Phi 1_{j,1}}{\Phi 1_{\text{floors},1}} \\ \phi 1 \end{array} \right.$$

$$\phi 2 := \left| \begin{array}{l} \text{for } j \in 1 .. \text{floors} \\ \quad \phi 2_{j,1} \leftarrow \dfrac{\Phi 2_{j,1}}{\Phi 2_{\text{floors},1}} \\ \phi 2 \end{array} \right.$$

$\phi 1 =$

	1
1	0.209
2	0.413
3	0.509
4	0.6
5	0.684
6	0.76
7	0.826
8	0.883
9	0.929
10	0.964
11	0.988
12	1

$\phi 2 =$

	1
1	0.209
2	0.413
3	0.509
4	0.6
5	0.684
6	0.76
7	0.826
8	0.883
9	0.929
10	0.964
11	0.988
12	1

Calculate SDOF equivalent mass:

$$em1 := \phi 1^{T} M1 \cdot \phi 1$$

$$em1 = 4.126 \times 10^{7} \text{ kg}$$

$$em2 := \phi 2^{T} M2 \cdot \phi 2$$

$$em2 = 2.986 \times 10^{7} \text{ kg}$$

Calculate frequency:

$$\omega 1 := \sqrt{\Lambda 1_{1,1}}$$

$$\Lambda 1_{1,1} = 279.75$$

$$\omega 1 = 16.726 \text{ radians/sec}$$

$$\omega 2 := \sqrt{\Lambda 2_{1,1}}$$

$$\Lambda 2_{1,1} = 87.723$$

$$\omega 2 = 9.366 \text{ radians/sec}$$

Calculate SDOF equivalent stiffness:

$$ek1 := em1 \cdot \omega 1^{2}$$

$$ek1 = 1.154 \times 10^{10} \text{ N/m}$$

$$ek2 := em2 \cdot \omega 2^{2}$$

$$ek2 = 2.619 \times 10^{9} \text{ N/m}$$

Optimized Stiffness and Damping for the Combined Structure

-This portion of the worksheet calculates the optimized stiffness and damping of a pair of equivalent SDOF systems based on the closed form solution of described in Richardson & Abdullah (2004).

-The equivalent properties of the walls calculated above will be used in the equations below. They will be renamed to coincide with the nomenclature used in the closed form solution.

$m1 := em1$ $m2 := em2$

$m1 = 4.126 \times 10^{7}$ kg $m2 = 2.986 \times 10^{7}$ kg

$k1 := ek1$ $k2 := ek2$

$k1 = 1.154 \times 10^{10}$ N/m $k2 = 2.619 \times 10^{9}$ N/m

$\omega 1 := \sqrt{\frac{k1}{m1}}$ $\omega 2 := \sqrt{\frac{k2}{m2}}$

$\omega 1 = 16.726$ radians/sec $\omega 2 = 9.366$ radians/sec

- A premise of using the closed form solution is that the natural frequency of building 1 is less than that of building 2. Using the natural frequencies found above, "if" statements will switch the building (wall) properties and redefine them as necessary.

$m1s := if(\omega 1 < \omega 2, m1, m2)$ $m1s = 2.986 \times 10^{7}$ kg

$m2s := if(\omega 1 < \omega 2, m2, m1)$ $m2s = 4.126 \times 10^{7}$ kg

$k1s := if(\omega 1 < \omega 2, k1, k2)$ $k1s = 2.619 \times 10^{9}$ N/m

$k2s := if(\omega 1 < \omega 2, k2, k1)$ $k2s = 1.154 \times 10^{10}$ N/m

$\omega 1s := if(\omega 1 < \omega 2, \omega 1, \omega 2)$ $\omega 1s = 9.366$ radians/sec

$\omega 2s := if(\omega 1 < \omega 2, \omega 2, \omega 1)$ $\omega 2s = 16.726$ radians/sec

The following variable indicates whether or not a switch took place:

$switch := if(\omega 1 < \omega 2, "No", "Yes")$ $switch = "Yes"$

Since dummy variable were used to switch the various properties above, the nomenclature must be reset to the original symbols used.

$m1 := m1s \qquad m2 := m2s$

$k1 := k1s \qquad k2 := k2s$

$\omega1 := \omega1s \qquad \omega2 := \omega2s$

The mass ratio:

$$\mu := \frac{m2}{m1} \qquad \mu = 1.382$$

The beginning of the Richardson/ Abdullah equations:

The closed form solution utilizes "g" in the calculation of η, but since the equation is so long, it will be split, using "g1" to shorten the equation for "g." This will be repeated later under similar circumstances.

$$g1 := \left(\mu^3\cdot\omega2^2 + 26\cdot\mu^2\cdot\omega2^2 + 9\cdot\mu^2\cdot\omega1^2 + 9\cdot\omega2^2\cdot\mu + 26\cdot\omega1^2\cdot\mu + \omega1^2\right)$$

$$g := \left(\omega2^2\cdot\mu + \omega1^2\right)\cdot g1\cdot\left(5\cdot\omega1^2 + 3\cdot\omega2^2 + \omega1^2\cdot\mu + 7\cdot\omega2^2\cdot\mu\right)^2$$

$$g = 1.826 \times 10^{14}$$

$$U1 := \left[\left(3\cdot\mu^5 + 15\cdot\mu^2 + 33\cdot\mu^3 + 21\cdot\mu^4\right)\cdot\omega2^4 - 3\cdot\sqrt{g} + \mu\cdot\sqrt{g}\right]\cdot\omega1^2$$

$$U2 := -3\cdot(\mu + 5)\cdot(\mu + 1)^2\cdot\omega1^6 - 3\cdot\omega2^2\cdot(7\cdot\mu + 3)\cdot(\mu + 1)^2\cdot\omega1^4 + U1$$

$$U := \frac{1}{4}\cdot(-\omega1 + \omega2)\cdot(\omega1 + \omega2)\cdot\left[U2 + \left(21\cdot\mu^5 + 51\cdot\mu^4 + 39\cdot\mu^3 + 9\cdot\mu^2\right)\cdot\omega2^6 + \left(3\cdot\mu^2\cdot\sqrt{g} - \mu\cdot\sqrt{g}\right)\cdot\omega2^2\right]\cdot\mu$$

$$U = 1.619 \times 10^{12}$$

$$L1 := \left(6\cdot\mu + \mu^2 + 5\right)\cdot\omega1^4 + \left(13\cdot\mu^2 + 3 + \mu^3 + 15\cdot\mu\right)\cdot\omega2^2\cdot\omega1^2$$

$$L := \left[\omega1^2\cdot(\mu + 1)^2\cdot\left(\omega2^2\cdot\mu + \omega1^2\right)\cdot\left[L1 + \left(7\cdot\mu^3 + 3\cdot\mu + 10\cdot\mu^2\right)\cdot\omega2^4 + \sqrt{g}\right]\right]$$

$$L = 4.283 \times 10^{12}$$

The fixed point stiffness ratio is calculated from U and L:

$$\eta := \frac{U}{L} \qquad \eta = 0.378$$

The natural frequency corresponding to the intersection at point "P" is calculated below:

$$Sp1 := 4\cdot\mu\cdot\omega1^2\cdot(\omega1-\omega2)\cdot(\omega1+\omega2)\cdot\left(\omega2^2\cdot\mu+\omega1^2\right)\cdot\left(-\mu^2\cdot\omega2^2+\omega2^2\cdot\mu+2\cdot\omega1^2\right)\cdot\eta$$

$$Sp := 4\cdot\omega1^4\cdot(\mu+1)^2\cdot\left(\omega2^2\cdot\mu+\omega1^2\right)^2\cdot\eta^2 - Sp1 + \mu^2\cdot(\omega1-\omega2)^2\cdot(\omega1+\omega2)^2\cdot\left(2\omega1^2+\omega2^2\cdot\mu\right)^2$$

$$Sp = 2.831\times10^{10}$$

$$\omega p1 := \left[\left[(3+2\cdot\eta)\cdot\omega2^2\cdot\omega1^2+\omega2^4\right]\cdot\mu^2+\left[(2+2\cdot\eta)\cdot\omega1^4+(2+2\cdot\eta)\cdot\omega2^2\cdot\omega1^2\right]\cdot\mu+2\cdot\omega1^4\cdot\eta-\sqrt{Sp}\right]$$

$$\omega p1 = 2.857\times10^{5}$$

$$\omega p := \frac{1}{2}\cdot\frac{\sqrt{2}\cdot\sqrt{\mu\cdot\left(\omega1^2\cdot\mu+\omega2^2\cdot\mu+2\cdot\omega1^2\right)\cdot\omega p1}}{\mu\cdot\left(\omega1^2\cdot\mu+\omega2^2\cdot\mu+2\cdot\omega1^2\right)}$$

$$\omega p = 12.301$$

The natural frequency corresponding to the intersection at point "Q" is calculated below:

$$Sq1 := 4\cdot\mu\cdot\omega1^2\cdot(\omega2-\omega1)\cdot(\omega1+\omega2)\cdot\left(\omega2^2\cdot\mu+\omega1^2\right)\cdot\left(2\cdot\mu^2\cdot\omega2^2+\omega1^2\cdot\mu-\omega1^2\right)\cdot\eta$$

$$Sq := 4\cdot\omega1^4\cdot(\mu+1)^2\cdot\left(\omega2^2\cdot\mu+\omega1^2\right)^2\cdot\eta^2 - Sq1 + \mu^2\cdot(\omega2-\omega1)^2\cdot(\omega1+\omega2)^2\cdot\left(2\cdot\omega2^2\cdot\mu+\omega1^2\right)^2$$

$$Sq = 3.938\times10^{10}$$

$$\omega q1 := \left[\left[(2+2\cdot\eta)\cdot\omega2^2\cdot\omega1^2+2\cdot\omega2^4\right]\cdot\mu^2+\left[(1+2\cdot\eta)\cdot\omega1^4+(3+2\cdot\eta)\cdot\omega2^2\cdot\omega1^2\right]\cdot\mu+2\cdot\omega1^4\cdot\eta+\sqrt{Sq}\right]$$

$$\omega q1 = 7.782\times10^{5}$$

$$\omega q := \frac{1}{2}\cdot\frac{\sqrt{2}\cdot\sqrt{\mu\cdot\left(2\cdot\omega2^2\cdot\mu+\omega2^2+\omega1^2\right)\cdot\omega q1}}{\mu\cdot\left(2\omega2^2\cdot\mu+\omega2^2+\omega1^2\right)}$$

$$\omega q = 15.714$$

The fixed point damping ratio corresponding to the "P" intersection point is calculated using the following set of equations. Richardson and Abdullah used xAx for components relating to point P:

$$aA := -32\cdot\omega p^{5}\cdot\omega 2^{12}\cdot\mu^{8}\cdot\omega 1^{8}(1+\mu)\left(\omega 1^{2}+\omega 2^{2}\cdot\mu\right)^{2}\cdot\left(-\omega 1^{2}-\omega 2^{2}\cdot\mu+\omega p^{2}+\omega p^{2}\cdot\mu\right)$$

$$aA = 2.072\times 10^{38}$$

$$bA1 := -2\cdot\omega p\cdot\mu^{4}\cdot\left(2\cdot\omega p^{4}\cdot\mu^{6}\cdot\omega 1^{8}\right)$$

$$bA1 = -1.692\times 10^{15}$$

$$bA2 := -2\cdot\omega p\cdot\mu^{4}\cdot\left[-8\cdot\mu^{5}\cdot\omega p^{2}(\eta+1)^{2}(1+\mu)\cdot\omega 1^{12}+4\cdot\omega p^{4}\cdot\mu^{5}\cdot(1+2\mu)(\eta+1)\cdot\omega 1^{10}-8\cdot\omega p^{6}\cdot\mu^{6}\cdot\omega 1^{8}\right]$$

$$bA2 = 1.036\times 10^{18}$$

"bA3" is split to include bA3a and bA3b:

$$bA3a := 2\cdot\omega p^{4}\cdot\mu^{4}\cdot\left[\left(4\cdot\mu^{2}+4+8\cdot\mu\right)\cdot\eta^{2}+\left(12\cdot\mu^{2}+10+28\cdot\mu\right)\cdot\eta+18\cdot\mu+7\cdot\mu^{2}+4\right]\cdot\omega 1^{12}$$

$$bA3b := -8\cdot\mu^{4}\cdot\omega p^{2}\cdot(\eta+1)\cdot(3\cdot\eta+1)\cdot(1+\mu)\cdot\omega 1^{14}$$

$$bA3 := -2\cdot\omega p\cdot\mu^{4}\cdot\left[bA3b+bA3a-8\cdot\omega p^{6}\cdot\mu^{5}\cdot(\mu\cdot\eta+\mu+2+\eta)\,\omega 1^{10}+6\cdot\omega p^{8}\cdot\mu^{6}\cdot\omega 1^{8}\right]$$

$$bA3 = -2.217\times 10^{20}$$

"bA4" is split to include bA4a, bA4aa and bA4b:

$$bA4aa := \left(4\cdot\mu^{2}+4+8\cdot\mu\right)\cdot\eta^{2}+\left(4+16\cdot\mu+9\cdot\mu^{2}\right)\cdot\eta+4\cdot\mu+2\cdot\mu^{2}$$

$$bA4a := -8\cdot\omega p^{2}\cdot\eta\cdot\mu^{3}\cdot(1+\mu)\cdot(2+3\cdot\eta)\cdot\omega 1^{16}+4\cdot\omega p^{4}\cdot\mu^{3}\cdot(bA4aa)\cdot\omega 1^{14}$$

$$bA4 := -2\cdot\omega p\cdot\mu^{4}\cdot\left[bA4a-8\cdot\omega p^{6}\cdot\mu^{4}\cdot\left(\mu^{2}\cdot\eta+\mu^{2}+4\cdot\mu+4\cdot\mu\cdot\eta+2+3\cdot\eta\right)\cdot\omega 1^{12}+12\cdot\omega p^{8}\cdot\mu^{5}\cdot\omega 1^{10}\right]$$

$$bA4 = 1.824\times 10^{22}$$

"bA5" is split to include bA5a and bA5b:

$$bA5a := -8\cdot\omega p^{6}\cdot\mu^{3}\cdot\left[\left(3\cdot\mu + \mu^{2} + 2\right)\cdot\eta + \mu\right]\cdot\omega 1^{14} + 2\cdot\mu^{4}\cdot\omega p^{8}\cdot\left(4 + 2\cdot\mu + \mu^{2}\right)\cdot\omega 1^{12}$$

$$bA5b := 4\cdot\omega p^{4}\cdot\eta\cdot\mu^{2}\cdot\left[\left(2\cdot\mu^{2} + 4\cdot\mu + 2\right)\cdot\eta + 3\cdot\mu^{2} + 4\cdot\mu\right]\cdot\omega 1^{16}$$

$$bA5 := -2\cdot\omega p\cdot\mu^{4}\cdot\left[-8\cdot\mu^{2}\cdot\omega p^{2}\cdot\eta^{2}\cdot(1 + \mu)\cdot\omega 1^{18} + bA5b + bA5a\right]$$

$$bA5 = -4.956 \times 10^{23}$$

$$bA := bA1\cdot\omega 2^{18} + bA2\cdot\omega 2^{16} + bA3\cdot\omega 2^{14} + bA4\cdot\omega 2^{12} + bA5\cdot\omega 2^{10}$$

$$bA = -7.189 \times 10^{35}$$

"cA" is split to include cA1, cA2 and cA3:

$$cA1 := \left[(1 + \eta)\cdot\omega 2^{4} + \left(-2\cdot\eta\cdot\omega p^{2} + \omega 1^{2}\cdot\eta^{2} - 2\cdot\omega p^{2} + \omega 1^{2}\cdot\eta\right)\cdot\omega 2^{2} + \omega p^{4}\right]\cdot\mu^{2}$$

$$cA1 = 5.126 \times 10^{4}$$

$$cA2 := \left[\omega 1^{4}\cdot\eta^{2} + \left(\eta^{2}\cdot\omega 2^{2} + 2\cdot\eta\cdot\omega 2^{2} - 2\cdot\eta\cdot\omega p^{2}\right)\cdot\omega 1^{2}\right]\cdot\mu$$

$$cA2 = 1.813 \times 10^{4}$$

$$cA3 := \left[\left[(1 + \eta)\cdot\omega 2^{2} - \omega p^{2}\right]\cdot\mu + \omega 1^{2}\cdot\eta\right]\cdot\left(cA1 + cA2 + \omega 1^{4}\cdot\eta^{2}\right)$$

$$cA3 = 2.515 \times 10^{7}$$

$$cA := 2\cdot\omega p\cdot\omega 2^{8}\cdot\mu^{4}\cdot\omega 1^{12}\cdot\left[(\omega p - \omega 2)\cdot(\omega p + \omega 2)\cdot\left(\omega p^{2} - \omega 1^{2}\cdot\eta - \omega 1^{2}\right)\cdot\mu + \omega 1^{4}\cdot\eta - \omega 1^{2}\cdot\eta\cdot\omega p^{2}\right]\cdot cA3$$

$$cA = -4.726 \times 10^{34}$$

The fixed point damping ratio corresponding to the "P" intersection point is calculated below:

$$\xi A := \sqrt{\frac{-bA + \sqrt{bA^{2} - 4\cdot aA\cdot cA}}{2\cdot aA}}$$

$$\xi A = 0.13$$

The fixed point damping ratio corresponding to the "Q" intersection point is calculated using the following set of equations. Richardson and Abdullah used xBx for components relating to point Q:

$$aB := -32\cdot\omega q^{5}\cdot\omega 2^{12}\cdot\mu^{8}\cdot\omega 1^{8}(1+\mu)\left(\omega 1^{2}+\omega 2^{2}\cdot\mu\right)^{2}\cdot\left(-\omega 1^{2}-\omega 2^{2}\cdot\mu+\omega q^{2}+\omega q^{2}\cdot\mu\right)$$

$$aB = -7.047\times 10^{38}$$

"bB1" is split to include bB1a:

$$bB1a := 4\cdot\omega q^{4}\cdot\mu^{5}\cdot(4\cdot\mu\cdot\eta+4\mu+2+3\cdot\eta)\cdot\omega 1^{10}$$

$$bB1 := -2\cdot\omega q\cdot\mu^{4}\cdot\left[-8\cdot\mu^{5}\cdot\omega q^{2}\cdot(\eta+1)^{2}\cdot(1+\mu)\cdot\omega 1^{12}+bB1a-8\cdot\omega q^{6}\cdot\mu^{6}\cdot\omega 1^{8}\right]$$

$$bB1 = 1.767\times 10^{17}$$

"bB2" is split to include bB2a, bB2b, and bB2c:

$$bB2a := -8\cdot\mu^{4}\cdot\omega q^{2}\cdot(\eta+1)\cdot(3\cdot\eta+1)\cdot(1+\mu)\cdot\omega 1^{14}$$

$$bB2b := -8\cdot\omega q^{6}\cdot\mu^{4}\cdot\left[\left(1+2\cdot\mu^{2}+3\cdot\mu\right)\cdot\eta+1+4\cdot\mu+2\cdot\mu^{2}\right]\cdot\omega 1^{10}+2\cdot\mu^{4}\cdot\omega q^{8}\cdot\left(4\cdot\mu^{2}+2\cdot\mu+1\right)\cdot\omega 1^{8}$$

$$bB2c := \left(32\cdot\mu+18+8\cdot\mu^{2}\right)\cdot\eta+18\cdot\mu+4\cdot\mu^{2}+7$$

$$bB2 := -2\cdot\omega q\cdot\mu^{4}\cdot\left[bB2a+2\cdot\omega q^{4}\cdot\mu^{4}\cdot\left[\left(4\cdot\mu^{2}+4+8\cdot\mu\right)\cdot\eta^{2}+bB2c\right]\cdot\omega 1^{12}+bB2b\right]$$

$$bB2 = 5.14\times 10^{19}$$

"bB3" is split to include bB3a and bB3b:

$$bB3a := 4\cdot\omega q^{4}\cdot\mu^{3}\cdot\left[\left(4\cdot\mu^{2}+4+8\cdot\mu\right)\cdot\eta^{2}+\left(6+14\cdot\mu+5\cdot\mu^{2}\right)\cdot\eta+2\cdot\mu+\mu^{2}\right]\cdot\omega 1^{14}$$

$$bB3b := -8\cdot\omega q^{2}\cdot\eta\cdot\mu^{3}\cdot(1+\mu)\cdot(2+3\cdot\eta)\cdot\omega 1^{16}+bB3a$$

$$bB3 := -2\cdot\omega q\cdot\mu^{4}\cdot\left[bB3b-8\cdot\omega q^{6}\cdot\mu^{3}\cdot\left(3\cdot\mu^{2}\cdot\eta+2\cdot\mu^{2}+\mu+4\cdot\mu\cdot\eta+\eta\right)\cdot\omega 1^{12}+12\cdot\omega q^{8}\cdot\mu^{5}\cdot\omega 1^{10}\right]$$

$$bB3 = -2.687\times 10^{22}$$

"bB4" is split to include bB4a and bB4b:

$$bB4a := 2\cdot\omega q^{4}\cdot\mu^{2}\cdot\left[\left(4\cdot\mu^{2}+8\cdot\mu+4\right)\cdot\eta^{2}+\left(2\cdot\mu^{2}+4\cdot\mu\right)\cdot\eta+\mu^{2}\right]\cdot\omega 1^{16}$$

$$bB4b := bB4a - 8\cdot\omega q^{6}\cdot\mu^{3}\cdot\left[(1+\mu)\cdot\eta+\mu\right]\cdot\omega 1^{14} + 6\cdot\mu^{4}\cdot\omega q^{8}\cdot\omega 1^{12}$$

$$bB4 := -2\cdot\omega q\cdot\mu^{4}\cdot\left[-8\cdot\mu^{2}\cdot\omega q^{2}\cdot\eta^{2}\cdot(1+\mu)\cdot\omega 1^{18}+bB4b\right]$$

$$bB4 = -1.69\times 10^{24}$$

$$bB := bB1\cdot\omega 2^{16} + bB2\cdot\omega 2^{14} + bB3\cdot\omega 2^{12} + bB4\cdot\omega 2^{10}$$

$$bB = -2.256\times 10^{36}$$

"cB" is split to include cBa, cBb, and cBc:

$$cBa := (\omega q-\omega 2)\cdot(\omega q+\omega 2)\cdot\left(\omega q^{2}-\omega 1^{2}\cdot\eta-\omega 1^{2}\right)\cdot\mu+\omega 1^{4}\cdot\eta-\omega 1^{2}\cdot\eta\cdot\omega q^{2}$$

$$cBb := (cBa)\cdot\left[\left(\omega 1^{2}\cdot\eta-\omega q^{2}+\omega 1^{2}\right)\cdot\omega 2^{2}\cdot\mu+\omega 1^{4}\cdot\eta\right]$$

$$cBc := \left[\left(\eta^{2}+\eta\right)\cdot\omega 1^{6}+\left(-2\cdot\eta\cdot\omega q^{2}+\eta^{2}\cdot\omega 2^{2}+\eta\cdot\omega 2^{2}\right)\cdot\omega 1^{4}\right]\cdot\mu+\omega 1^{6}\cdot\eta^{2}$$

$$cB := 2\cdot\omega q\cdot\omega 1^{8}\cdot\mu^{4}\cdot\omega 2^{8}\cdot cBb\cdot\left[\omega 2^{2}\cdot\left(\omega q^{2}-\omega 1^{2}\cdot\eta-\omega 1^{2}\right)^{2}\cdot\mu^{2}+cBc\right]$$

$$cB = 1.806\times 10^{35}$$

The fixed point damping ratio corresponding to the "Q" intersection point is calculated below:

$$\xi B := \sqrt{\frac{-bB-\sqrt{bB^{2}-4\cdot aB\cdot cB}}{2\cdot aB}}$$

$$\xi B = 0.12$$

The average damping ratio is calculated below:

$$\xi := \frac{\xi A+\xi B}{2}$$

$$\xi = 0.125$$

Results Summary

The equivalent SDOF weight and stiffness:

$m1 = 2.986 \times 10^{7}$ kg

$m2 = 4.126 \times 10^{7}$ kg

$\mu = 1.382$

$k1 = 2.619 \times 10^{9}$ N/m

$k2 = 1.154 \times 10^{10}$ N/m

The optimal stiffness is calculated using the fixed point stiffness ratio:

$\eta = 0.378$

$kfp := k1 \cdot \eta$

$kfp = 9.901 \times 10^{8}$ N/m

The ratio of the natural frequencies is calculated by ωratio below:

$$\omega ratio := \frac{\omega 2}{\omega 1}$$

$\omega ratio = 1.786$

The optimal damping ratio values:

Point P damping ratio:

$\xi A = 0.13$

Point P damping ratio:

$\xi B = 0.12$

Optimal system damping ratio:

$\xi = 0.125$

APPENDIX B

TABULATED DATA FOR WALL COMBINATION TRIALS

Case 1 (12 Stories, No Wall Pier Cracking)

Case 2 (24 Stories, No Wall Pier Cracking)

Case 3 (12 Stories, Wall Pier Cracking)

Case 4 (24 Stories, Wall Pier Cracking)

Table B.1
Case 1 (12 Stories, Uncracked)

	Properties of Equivalent SDOF Representations of Wall Piers (Seto et al. 1987)										Calculated Optimal Coupling Properties (Richardson and Abdullah 2006)			
Trial # [1]	Wall 1 [2,3]	m1 (kg)	k1 (N/m)	ω1 (Hz)	Wall 2 [2,3]	m2 (kg)	k2 (N/m)	ω2 (Hz)	Mass Ratio μ	Frequency Ratio γ	Coupling Damping Ratio ξ	Damping c_d (Ns/m)	Coupling Stiffness Ratio η	Coupling Stiffness k (N/m)
1 - 1	B12	2.42E+07	2.49E+10	5.103	A12	3.86E+07	5.79E+10	6.167	1.59	1.21	0.047	1.41E+08	0.067	1.66E+09
1 - 2	C12	1.92E+07	7.73E+09	3.192	A12	4.35E+07	5.79E+10	5.803	2.27	1.82	0.081	2.59E+08	0.698	5.39E+09
1 - 3	D12	2.53E+07	1.93E+10	4.395	A12	3.75E+07	5.79E+10	6.254	1.48	1.42	0.083	2.46E+08	0.160	3.08E+09
1 - 4	E12	2.06E+07	4.37E+09	2.320	A12	4.22E+07	5.79E+10	5.896	2.05	2.54	0.112	3.50E+08	1.674	7.32E+09
1 - 5	F12	1.62E+07	3.34E+09	2.285	A12	4.65E+07	5.79E+10	5.612	2.87	2.46	0.077	2.53E+08	1.950	6.51E+09
1 - 6	G12	2.63E+07	1.17E+10	3.354	A12	3.65E+07	5.79E+10	6.340	1.39	1.89	0.132	3.84E+08	0.466	5.44E+09
1 - 7	C12	2.59E+07	7.73E+09	2.749	B12	3.68E+07	2.49E+10	4.135	1.42	1.50	0.096	1.84E+08	0.195	1.51E+09
1 - 8	D12	3.25E+07	1.93E+10	3.876	B12	3.03E+07	2.49E+10	4.563	0.93	1.18	0.059	1.02E+08	0.006	1.23E+08
1 - 9	E12	2.74E+07	4.37E+09	2.009	B12	3.53E+07	2.49E+10	4.224	1.29	2.10	0.153	2.87E+08	0.599	2.62E+09
1 - 10	F12	2.24E+07	3.34E+09	1.944	B12	4.04E+07	2.49E+10	3.951	1.80	2.03	0.112	2.24E+08	0.799	2.67E+09
1 - 11	G12	3.35E+07	1.17E+10	2.969	B12	2.92E+07	2.49E+10	4.644	0.87	1.56	0.143	2.44E+08	0.074	8.60E+08
1 - 12	C12	2.48E+07	7.73E+09	2.808	D12	3.79E+07	1.93E+10	3.588	1.53	1.28	0.061	1.04E+08	0.091	7.07E+08
1 - 13	E12	3.29E+07	4.37E+09	1.834	C12	2.98E+07	7.73E+09	2.563	0.90	1.40	0.111	1.07E+08	0.039	1.68E+08
1 - 14	F12	2.77E+07	3.34E+09	1.749	C12	3.51E+07	7.73E+09	2.362	1.27	1.35	0.083	8.60E+07	0.089	2.98E+08
1 - 15	G12	3.89E+07	1.17E+10	2.756	C12	2.38E+07	7.73E+09	2.866	0.61	1.04	0.017	1.49E+07	-0.005	-5.97E+07
1 - 16	E12	2.63E+07	4.37E+09	2.051	D12	3.64E+07	1.93E+10	3.662	1.38	1.79	0.125	2.10E+08	0.378	1.65E+09
1 - 17	F12	2.14E+07	3.34E+09	1.990	D12	4.14E+07	1.93E+10	3.435	1.94	1.73	0.090	1.61E+08	0.505	1.69E+09
1 - 18	G12	3.24E+07	1.17E+10	3.020	D12	3.03E+07	1.93E+10	4.012	0.94	1.33	0.095	1.46E+08	0.029	3.43E+08
1 - 19	E12	3.66E+07	4.37E+09	1.739	F12	2.61E+07	3.34E+09	1.800	0.71	1.03	0.014	8.55E+06	-0.003	-1.45E+07
1 - 20	E12	2.53E+07	4.37E+09	2.091	G12	3.74E+07	1.17E+10	2.811	1.48	1.34	0.073	9.62E+07	0.117	5.12E+08
1 - 21	F12	2.04E+07	3.34E+09	2.035	G12	4.23E+07	1.17E+10	2.644	2.07	1.30	0.050	6.97E+07	0.158	5.27E+08

1. Trial number: X-YY; where X = Case 1 through 4 (described in Section 3.1); and YY = trial combination 1 through 21
2. Walls 1 and 2 have been designated such that $\gamma = \omega 2/\omega 1 > 1.0$ as discussed in Section 2.3.2.
3. Wall designations indicate the wall pattern, A through G (see Table 3.1) and the number of stories, 12 or 24.
4. The solution method employed is unstable as $\mu\gamma$ approaches 1.0. This is discussed in Section 3.3. Solutions where $\gamma < 1.05$ are not considered stable and are not considered further in this work.

$$\omega = \sqrt{\frac{k}{m}} \qquad \mu = \frac{m_2}{m_1}$$

$$\gamma = \frac{\omega 2}{\omega 1} > 1.0 \qquad c_d = \xi \cdot 2 \cdot \sqrt{m_2 k_2} \qquad \eta = \frac{k}{k_1}$$

Table B.2
Case 2 (24 Stories, Uncracked)

	Properties of Equivalent SDOF Representations of Wall Piers (Seto et al. 1987)										Calculated Optimal Coupling Properties (Richardson and Abdullah 2006)			
Trial #[1]	Wall 1 [2,3]	m1 (kg)	k1 (N/m)	ω1 (Hz)	Wall 2 [2,3]	m2 (kg)	k2 (N/m)	ω2 (Hz)	Mass Ratio μ	Frequency Ratio γ	Coupling Damping Ratio ξ	Damping c_d (Ns/m)	Coupling Stiffness Ratio η	Coupling Stiffness k (N/m)
2 - 1	B24	4.73E+07	1.27E+10	2.605	A24	7.53E+07	2.95E+10	3.148	1.59	1.21	0.047	1.40E+08	0.067	8.45E+08
2 - 2	C24	3.75E+07	3.93E+09	1.629	A24	8.51E+07	2.95E+10	2.962	2.27	1.82	0.081	2.58E+08	0.698	2.74E+09
2 - 3	D24	4.94E+07	9.81E+09	2.244	A24	7.32E+07	2.95E+10	3.192	1.48	1.42	0.083	2.45E+08	0.160	1.57E+09
2 - 4	E24	4.02E+07	2.23E+09	1.184	A24	8.24E+07	2.95E+10	3.010	2.05	2.54	0.112	3.49E+08	1.674	3.73E+09
2 - 5	F24	3.17E+07	1.70E+09	1.166	A24	9.10E+07	2.95E+10	2.865	2.87	2.46	0.077	2.53E+08	1.950	3.32E+09
2 - 6	G24	5.14E+07	5.94E+09	1.712	A24	7.13E+07	2.95E+10	3.237	1.39	1.89	0.132	3.83E+08	0.466	2.77E+09
2 - 7	C24	5.06E+07	3.93E+09	1.403	B24	7.20E+07	1.27E+10	2.111	1.42	1.50	0.096	1.84E+08	0.195	7.69E+08
2 - 8	D24	6.35E+07	9.81E+09	1.978	B24	5.91E+07	1.27E+10	2.329	0.93	1.18	0.059	1.01E+08	0.006	6.25E+07
2 - 9	E24	5.36E+07	2.23E+09	1.026	B24	6.90E+07	1.27E+10	2.156	1.29	2.10	0.153	2.87E+08	0.599	1.33E+09
2 - 10	F24	4.38E+07	1.70E+09	0.992	B24	7.89E+07	1.27E+10	2.017	1.80	2.03	0.112	2.23E+08	0.799	1.36E+09
2 - 11	G24	6.55E+07	5.94E+09	1.516	B24	5.71E+07	1.27E+10	2.371	0.87	1.56	0.143	2.44E+08	0.074	4.38E+08
2 - 12	C24	4.85E+07	3.93E+09	1.433	D24	7.41E+07	9.81E+09	1.831	1.53	1.28	0.061	1.04E+08	0.091	3.60E+08
2 - 13	E24	6.44E+07	2.23E+09	0.936	C24	5.82E+07	3.93E+09	1.308	0.90	1.40	0.111	1.07E+08	0.039	8.57E+07
2 - 14	F24	5.41E+07	1.70E+09	0.893	C24	6.85E+07	3.93E+09	1.206	1.27	1.35	0.083	8.58E+07	0.089	1.52E+08
2 - 15	G24	7.61E+07	5.94E+09	1.407	C24	4.66E+07	3.93E+09	1.463	0.61	1.04	0.017	1.48E+07	-0.005	-3.04E+07
2 - 16	E24	5.15E+07	2.23E+09	1.047	D24	7.11E+07	9.81E+09	1.869	1.38	1.79	0.125	2.09E+08	0.378	8.42E+08
2 - 17	F24	4.18E+07	1.70E+09	1.016	D24	8.09E+07	9.81E+09	1.753	1.94	1.73	0.090	1.60E+08	0.505	8.58E+08
2 - 18	G24	6.34E+07	5.94E+09	1.541	D24	5.93E+07	9.81E+09	2.048	0.94	1.33	0.095	1.45E+08	0.029	1.75E+08
2 - 19	E24	7.16E+07	2.23E+09	0.888	F24	5.11E+07	1.70E+09	0.919	0.71	1.03	0.014	8.53E+06	-0.003	-7.36E+06
2 - 20	E24	4.95E+07	2.23E+09	1.067	G24	7.31E+07	5.94E+09	1.435	1.48	1.34	0.073	9.60E+07	0.117	2.61E+08
2 - 21	F24	3.99E+07	1.70E+09	1.039	G24	8.27E+07	5.94E+09	1.349	2.07	1.30	0.050	6.96E+07	0.158	2.69E+08

1. Trial number: X-YY; where X = Case 1 through 4 (described in Section 3.1); and YY = trial combination 1 through 21
2. Walls 1 and 2 have been designated such that $\gamma = \omega 2/\omega 1 > 1.0$ as discussed in Section 2.3.2.
3. Wall designations indicate the wall pattern, A through G (see Table 3.1) and the number of stories, 12 or 24.
4. The solution method employed is unstable as μ approaches 1.0. This is discussed in Section 3.3. Solutions where $\gamma < 1.05$ are not considered stable and are not considered further in this work.

$$\omega = \sqrt{\frac{k}{m}} \qquad \mu = \frac{m_2}{m_1}$$

$$\gamma = \frac{\omega 2}{\omega 1} > 1.0 \qquad c_d = \xi \cdot 2 \cdot \sqrt{m_2 k_2} \qquad \eta = \frac{k}{k_1}$$

Table B.3
Case 3 (12 Stories, Cracked)

	Properties of Equivalent SDOF Representations of Wall Piers (Seto et al. 1987)										Calculated Optimal Coupling Properties (Richardson and Abdullah 2006)			
Trial #[1]	Wall 1[2,3]	m1 (kg)	k1 (N/m)	ω1 (Hz)	Wall 2[2,3]	m2 (kg)	k2 (N/m)	ω2 (Hz)	Mass Ratio μ	Frequency Ratio γ	Coupling Damping Ratio ξ	Damping c_d (Ns/m)	Coupling Stiffness Ratio η	Coupling Stiffness k (N/m)
3 - 1	B12	2.74E+07	1.49E+10	3.710	A12	4.37E+07	3.47E+10	4.483	1.59	1.21	0.047	1.16E+08	0.067	9.94E+08
3 - 2	C12	2.18E+07	4.63E+09	2.320	A12	4.93E+07	3.47E+10	4.219	2.27	1.82	0.081	2.13E+08	0.698	3.23E+09
3 - 3	D12	2.86E+07	1.15E+10	3.195	A12	4.25E+07	3.47E+10	4.546	1.48	1.42	0.083	2.02E+08	0.160	1.85E+09
3 - 4	**E12**	**2.33E+07**	**2.62E+09**	**1.687**	**A12**	**4.78E+07**	**3.47E+10**	**4.286**	**2.05**	**2.54**	**0.112**	**2.88E+08**	**1.674**	**4.38E+09**
3 - 5	F12	1.84E+07	2.00E+09	1.661	A12	5.27E+07	3.47E+10	4.080	2.87	2.46	0.077	2.09E+08	1.950	3.90E+09
3 - 6	G12	2.98E+07	6.99E+09	2.438	A12	4.13E+07	3.47E+10	4.609	1.39	1.89	0.132	3.16E+08	0.466	3.26E+09
3 - 7	C12	2.94E+07	4.63E+09	1.998	B12	4.18E+07	1.49E+10	3.006	1.42	1.50	0.096	1.52E+08	0.195	9.05E+08
3 - 8	D12	3.68E+07	1.15E+10	2.817	B12	3.43E+07	1.49E+10	3.317	0.93	1.18	0.059	8.36E+07	0.006	7.35E+07
3 - 9	E12	3.11E+07	2.62E+09	1.460	B12	4.00E+07	1.49E+10	3.071	1.29	2.10	0.153	2.37E+08	0.599	1.57E+09
3 - 10	F12	2.54E+07	2.00E+09	1.413	B12	4.57E+07	1.49E+10	2.872	1.80	2.03	0.112	1.84E+08	0.799	1.60E+09
3 - 11	G12	3.80E+07	6.99E+09	2.158	B12	3.31E+07	1.49E+10	3.376	0.87	1.56	0.143	2.01E+08	0.074	5.15E+08
3 - 12	C12	2.81E+07	4.63E+09	2.041	D12	4.30E+07	1.15E+10	2.608	1.53	1.28	0.061	8.56E+07	0.091	4.23E+08
3 - 13	E12	3.73E+07	2.62E+09	1.333	C12	3.38E+07	4.63E+09	1.863	0.90	1.40	0.111	8.81E+07	0.039	1.01E+08
3 - 14	F12	3.14E+07	2.00E+09	1.271	C12	3.98E+07	4.63E+09	1.717	1.27	1.35	0.083	7.09E+07	0.089	1.78E+08
3 - 15	G12	4.41E+07	6.99E+09	2.004	C12	2.70E+07	4.63E+09	2.083	0.61	1.04	0.017	1.23E+07	-0.005	-3.58E+07
3 - 16	**E12**	**2.99E+07**	**2.62E+09**	**1.491**	**D12**	**4.13E+07**	**1.15E+10**	**2.662**	**1.38**	**1.79**	**0.125**	**1.73E+08**	**0.378**	**9.90E+08**
3 - 17	F12	2.42E+07	2.00E+09	1.447	D12	4.69E+07	1.15E+10	2.497	1.94	1.73	0.090	1.32E+08	0.505	1.01E+09
3 - 18	G12	3.67E+07	6.99E+09	2.195	D12	3.44E+07	1.15E+10	2.916	0.94	1.33	0.095	1.20E+08	0.029	2.06E+08
3 - 19	E12	4.15E+07	2.62E+09	1.264	F12	2.96E+07	2.00E+09	1.308	0.71	1.03	0.014	7.04E+06	-0.003	-8.66E+06
3 - 20	E12	2.87E+07	2.62E+09	1.520	G12	4.24E+07	6.99E+09	2.043	1.48	1.34	0.073	7.93E+07	0.117	3.07E+08
3 - 21	F12	2.32E+07	2.00E+09	1.479	G12	4.79E+07	6.99E+09	1.922	2.07	1.30	0.050	5.75E+07	0.158	3.16E+08

1. Trial number: X-YY; where X = Case 1 through 4 (described in Section 3.1); and YY = trial combination 1 through 21
2. Walls 1 and 2 have been designated such that $\gamma = \omega 2/\omega 1 > 1.0$ as discussed in Section 2.3.2.
3. Wall designations indicate the wall pattern, A through G (see Table 3.1) and the number of stories, 12 or 24.
4. The solution method employed is unstable as μ approaches 1.0. This is discussed in Section 3.3. Solution where $\gamma < 1.05$ are not considered stable and are not considered further in this work.

$$\omega = \sqrt{\frac{k}{m}}$$

$$\mu = \frac{m_2}{m_1}$$

$$\gamma = \frac{\omega 2}{\omega 1} > 1.0$$

$$c_d = \xi \cdot 2 \cdot \sqrt{m_2 k_2}$$

$$\eta = \frac{k}{k_1}$$

Table B.4
Case 4 (24 Stories, Cracked)

	Properties of Equivalent SDOF Representations of Wall Piers (Seto et al. 1987)										Calculated Optimal Coupling Properties (Richardson and Abdullah 2006)			
Trial #[1]	Wall 1 [2,3]	m1 (kg)	k1 (N/m)	ω1 (Hz)	Wall 2 [2,3]	m2 (kg)	k2 (N/m)	ω2 (Hz)	Mass Ratio μ	Frequency Ratio γ	Coupling Damping Ratio ξ	Damping c_d (Ns/m)	Coupling Stiffness Ratio η	Coupling Stiffness k (N/m)
4 - 1	B24	5.24E+07	7.87E+09	1.949	A24	8.36E+07	1.83E+10	2.356	1.59	1.21	0.047	1.17E+08	0.067	5.25E+08
4 - 2	C24	4.16E+07	2.44E+09	1.219	A24	9.44E+07	1.83E+10	2.217	2.27	1.82	0.081	2.14E+08	0.698	1.71E+09
4 - 3	D24	5.48E+07	6.10E+09	1.679	A24	8.12E+07	1.83E+10	2.389	1.48	1.42	0.083	2.03E+08	0.160	9.76E+08
4 - 4	E24	4.46E+07	1.38E+09	0.886	A24	9.14E+07	1.83E+10	2.252	2.05	2.54	0.112	2.90E+08	1.674	2.32E+09
4 - 5	F24	3.51E+07	1.06E+09	0.873	A24	1.01E+08	1.83E+10	2.144	2.87	2.46	0.077	2.10E+08	1.950	2.06E+09
4 - 6	G24	5.70E+07	3.69E+09	1.281	A24	7.90E+07	1.83E+10	2.422	1.39	1.89	0.132	3.18E+08	0.466	1.72E+09
4 - 7	C24	5.62E+07	2.44E+09	1.050	B24	7.99E+07	7.87E+09	1.580	1.42	1.50	0.096	1.53E+08	0.195	4.78E+08
4 - 8	D24	7.04E+07	6.10E+09	1.481	B24	6.56E+07	7.87E+09	1.743	0.93	1.18	0.059	8.41E+07	0.006	3.88E+07
4 - 9	E24	5.95E+07	1.38E+09	0.768	B24	7.65E+07	7.87E+09	1.614	1.29	2.10	0.153	2.38E+08	0.599	8.28E+08
4 - 10	F24	4.85E+07	1.06E+09	0.743	B24	8.75E+07	7.87E+09	1.509	1.80	2.03	0.112	1.85E+08	0.799	8.44E+08
4 - 11	G24	7.27E+07	3.69E+09	1.134	B24	6.33E+07	7.87E+09	1.774	0.87	1.56	0.143	2.02E+08	0.074	2.72E+08
4 - 12	C24	5.38E+07	2.44E+09	1.073	D24	8.22E+07	6.10E+09	1.371	1.53	1.28	0.061	8.60E+07	0.091	2.24E+08
4 - 13	E24	7.14E+07	1.38E+09	0.701	C24	6.46E+07	2.44E+09	0.979	0.90	1.40	0.111	8.86E+07	0.039	5.33E+07
4 - 14	F24	6.00E+07	1.06E+09	0.668	C24	7.60E+07	2.44E+09	0.902	1.27	1.35	0.083	7.12E+07	0.089	9.41E+07
4 - 15	G24	8.44E+07	3.69E+09	1.053	C24	5.17E+07	2.44E+09	1.095	0.61	1.04	0.017	1.23E+07	-0.005	-1.89E+07
4 - 16	E24	5.71E+07	1.38E+09	0.783	D24	7.89E+07	6.10E+09	1.399	1.38	1.79	0.125	1.74E+08	0.378	5.23E+08
4 - 17	F24	4.63E+07	1.06E+09	0.760	D24	8.97E+07	6.10E+09	1.312	1.94	1.73	0.090	1.33E+08	0.505	5.33E+08
4 - 18	G24	7.03E+07	3.69E+09	1.154	D24	6.57E+07	6.10E+09	1.533	0.94	1.33	0.095	1.21E+08	0.029	1.09E+08
4 - 19	E24	7.94E+07	1.38E+09	0.665	F24	5.66E+07	1.06E+09	0.687	0.71	1.03	0.014	7.08E+06	-0.003	-4.57E+06
4 - 20	E24	5.49E+07	1.38E+09	0.799	G24	8.11E+07	3.69E+09	1.074	1.48	1.34	0.073	7.97E+07	0.117	1.62E+08
4 - 21	F24	4.43E+07	1.06E+09	0.777	G24	9.17E+07	3.69E+09	1.010	2.07	1.30	0.050	5.77E+07	0.158	1.67E+08

1. Trial number: X-YY; where X = Case 1 through 4 (described in Section 3.1); and YY = trial combination 1 through 21
2. Walls 1 and 2 have been designated such that $\gamma = \omega 2/\omega 1 > 1.0$ as discussed in Section 2.3.2.
3. Wall designations indicate the wall pattern, A through G (see Table 3.1) and the number of stories, 12 or 24.
4. The solution method employed is unstable as μ approaches 1.0. This is discussed in Section 3.3. Solutions where $\gamma < 1.05$ are not considered stable and are not considered further in this work.

$$\omega = \sqrt{\frac{k}{m}} \qquad \mu = \frac{m_2}{m_1}$$

$$\gamma = \frac{\omega 2}{\omega 1} > 1.0 \qquad c_d = \xi \cdot 2 \cdot \sqrt{m_2 k_2} \qquad \eta = \frac{k}{k_1}$$

REFERENCES

ACI Committee 318, 2005. *ACI 318-05/ACI 318R-05 Building Code Requirements for Reinforced Concrete and Commentary*, American Concrete Institute. Farmington Hills MI.

American Society of Civil Engineers (ASCE), 2002. *SEI/ASCE 7 – Minimum Design Loads for Buildings and Other Structures*, American Society of Civil Engineers, Reston, VA.

Carr, A., 2000. RUAUMOKO - Inelastic Dynamic Analysis Computer Program. University of Canterbury.

Federal Emergency Management Agency (FEMA), 2000. *FEMA 356 – Prestandard and Commentary for the Seismic Rehabilitation of Buildings*, Washington, D.C.

Harries, K.A., 2001. Ductility and Deformability of Coupling Beams in Reinforced Concrete Coupled Walls, *Earthquake Spectra*, Vol. 17, No. 3, August 2001 pp 457-478.

Harries, K.A., Fortney, P., Shahrooz, B.M. and Brienen, P., 2005. Design of Practical Diagonally Reinforced Concrete Coupling Beams – A Critical Review of ACI 318 Requirements, *ACI Structures Journal*. Vol. 102, No. 6, pp 876-882.

Harries, K.A., Gong B. and Shahrooz, B., 2000, Behavior and Design of Reinforced Concrete, Steel and Steel-Concrete Coupling Beams, *Earthquake Spectra*, Vol. 16, No. 4, November 2000, pp 775-800.

Harries, K.A. and McNeice, D.S. 2006. Performance-Based Design of High-Rise Coupled Wall Systems, *The Structural Design of Tall and Special Structures* (in press)

Harries, K.A., Moulton, D. and Clemson, R., 2004a. Parametric Study of Coupled Wall Behavior – Implications for the Design of Coupling Beams. *ASCE Journal of Structural Engineering* Vol. 130, No. 3 pp 480-488

Harries, K.A., Shahrooz, B., 2005. Hybrid Coupled Wall Systems, *Concrete International*. Vol. 27, No. 5, May 2005, pp 45-51.

Harries, K.A., Shahrooz, B.M., Brienen, P. and Fortney, P. 2004b. Performance Based Design of Coupled Walls. *Proceedings of the 5th International Conference on Composite Construction*, South Africa, July 2004.

Iwanami, K., Suzuki, K., Seto, K., 1996. Vibration Control Method for Parallel Structures Connected by Damper and Spring, *JSME International Journal*, Vol. 39, No. 4, pp 714-720.

Minami, S., Yamazaki, S., Toyama, K., Tahara, K., 2004. Experimental Study on Coupled Vibration Control Structures, *13th World Conference on Earthquake Engineering*, Vancouver, paper # 2351.

Naeim, F., 2003. *The Seismic Design Handbook* – 2nd Ed. Kluwer Academic Publishers.

Newmark, N.M. and Hall, W.J., 1982. *Earthquake Spectra and Design*, EERI, 103 pp.

Park, R. and Paulay, T., 1975. *Reinforced Concrete Structures*, John Wiley and Sons, Inc., New York 769 pp.

Paulay, T., 1971. Coupling Beams of Reinforced Concrete Shear Walls, *ASCE Journal of the Structural Division*, Vol. 97, No. ST 3, pp 843-862.

Richardson, A., 2003. *Vibration Control of Multiple Structures – Theory and Application.* Ph.D. dissertation, Florida A&M University. 286 pp.

Seto, K., Ookuma, M., Yamashita, S., Nagamatsu, A., 1987. Method of Estimating Equivalent Mass of Multi-Degree-of-Freedom System, *JSME International Journal*, Vol. 30, No. 268, pp 1638-1644.

Shahrooz, B.M., Harries, K.A. and Rassati, G.A., 2006. *NEESR-II: Hybrid Testing and Model Based Simulation for Performance-Based Design of Coupled Walls* Research Proposal submitted to the National Science Foundation, January 2006.

Stafford-Smith, B. and Coull, A., 1991. *Tall Building Structures – Analysis and Design.* Wiley Interscience.

Tedesco, J.W., McDougal, W.G., Ross, C.A., 1999. *Structural Dynamics – Theory and Applications*. Addison Wesley Longman.